Rainfall validates MODIS-derived NDVI as an index of spatio-temporal variation in green biomass across non-montane semi-arid and arid Central Asia

Adam Formica[1*], **Robert J. Burnside**[2] **& Paul M. Dolman**[2]

[1]*School of Geography and the Environment, University of Oxford, South Parks Road, Oxford, OX1 3QY, UK.*

[2]*School of Environmental Sciences, University of East Anglia, Norwich Research Park, Norwich, Norfolk, NR4 7TJ, UK.*

Corresponding author: adamformica@gmail.com

Word count: *c* 6865 (incl. Abstract, Main text, References)

Figures: 7, Tables: 1

Abstract

As satellite-derived normalized difference vegetation index (NDVI) is related to vegetation biomass, it may provide a proxy for habitat quality across extensive species ranges where ground-truth data are scarce. However, NDVI may have limited accuracy in sparsely-vegetated arid and semi-arid environments due to signal contamination by substrate reflectance. To validate NDVI as a vegetation proxy in the low-altitude deserts of Central Asia, we examine its response to precipitation across the migratory corridor of Asian Houbara *Chlamydotis macqueenii*, a threatened gamebird occupying deserts from the Middle East to China. Restricting NDVI data by altitude (masking higher elevations unoccupied by n=61 satellite-tracked houbara) and 2009 Globcover land cover (excluding cropland and built-up area), we relate moderate-resolution imaging spectroradiometer (MODIS) NDVI data to Global Precipitation Climatology Project precipitation data across five World Wildlife Fund semi-arid ecoregions (totaling 4.06 million km^2). We examine this both spatially (per 1 degree cell, mean annual NDVI and mean precipitation over 16 years, 2000–2015); and temporally (annual NDVI and annual precipitation) using separate temporal General Linear Models per cell and an overall Generalized Linear Mixed Model (GLMM) (including cell ID as a random effect). We sought to explain spatial variation in the NDVI-precipitation relation among temporal per degree-cell models, in terms of the slope (strength) and adjusted (adj.) R^2 (explanatory power), using inter-annual mean NDVI (2000–2015) and Gridded Livestock of the World livestock density. NDVI increases with precipitation, both spatially (adj. R^2 = 0.58, $p < 0.001$) and temporally (mean adj. R^2 across n=244, 1 degree cells = 0.44; GLMM across cells $p < 0.001$). More vegetated regions show a

stronger temporal response of vegetation biomass for a given precipitation increment (slope of NDVI to precipitation in per cell temporal models increases with inter-annual mean NDVI; adj. $R^2 = 0.38$, $p < 0.001$), reinforcing the conclusion that NDVI provides a proxy for vegetation abundance. The slope of this relation did not differ among ecoregions. Although livestock density is generally assumed to degrade vegetation and weaken the NDVI-precipitation relationship, explanatory power (adj. R^2 of per cell NDVI-precipitation models) is weakly, but positively, related to livestock density (adj. $R^2 = 0.02$, $p = 0.011$). This may be because we assess livestock at a coarse grain, at scales where overall stocking density is positively associated with vegetation abundance, but may also indicate that livestock are not degrading vegetation at regional landscape-scales despite potential localized effects. The strong signature of rainfall shows MODIS NDVI offers a potentially powerful proxy for spatial and temporal variation in arid and semi-arid vegetation at a resolution of 1 degree and 1 year over the houbara's breeding and wintering range, and probably also at finer spatial resolutions. NDVI can therefore be used in analyses relating (a) staging and wintering site selection to variation in habitat among potential wintering locations, and (b) variation within and between localities to demographic carry-over effects.

Keywords: NDVI, validation, precipitation, Asian Houbara, extensive grazing, pastoralism

1. Introduction

The Normalized Difference Vegetation Index (NDVI) is a remotely sensed, freely-available proxy for green leaf biomass and leaf area index, related to primary productivity (Tucker and Sellers, 1986). It supports a mechanistic understanding of how species respond to climatic and environmental change, thus offering predictive potential. Global coverage and multi-decadal timespans make NDVI data a powerful ecological tool (Pettorelli et al., 2011, 2005) which has helped explain migration patterns (Bridge et al., 2016; Saino 2004a; Tøttrup et al., 2008), life history traits (Saino et al., 2004) and avian survival (Grande et al., 2009; Schaub et al., 2005). As NDVI responds to climatic and environmental change, it can be used to predict how changing precipitation under future climate scenarios may affect vegetation structure and productivity (Yang et al. 2014), and thus habitat quality and species distributions (Hu and Jiang, 2011; Singh and Milner-Gulland, 2011). However, the information content and explanatory power of NDVI as a proxy for vegetation productivity, indicated by the degree of correlation with precipitation (Weiss et al., 2004) or soil moisture (Yang et al. 2014), can vary geographically owing to varying signal contamination by background reflectance. Geographic inconsistency in NDVI performance makes it problematic for measuring climatic and environmental change, or as a consistent predictor of species distributions when considered at inter-regional rather than localized scales. Lower accuracy in some areas may cause the link between NDVI and species distributions to break down (Parra et al., 2004; Pettorelli et al., 2006). Consequently, the performance of NDVI should be validated across relevant spatial extents, prior to use in ecological research.

NDVI signal contamination from canopy gaps and background conditions can vary with precipitation gradients, snowfall, litterfall, soil organic matter content and substrate mineralogy (Huete et al., 1999), so that the responsiveness of NDVI to vegetation productivity varies geographically. NDVI is affected by differences in soil brightness even for constant vegetation cover, particularly when this is less than 50% (Huete et al., 1985). Therefore, NDVI may have limited application in sparsely-vegetated arid and semi-arid environments with abundant exposed substrate, even though problems from clouds, atmospheric effects, and signal saturation are less in such regions (Gamon et al., 1995; Kaufman et al., 1992). However, as many desert species are sparsely distributed over large ranges, making it challenging to obtain extensive field-based measures to model occupancy, demographic performance and thus habitat suitability, the potential to use NDVI as a proxy could be extremely valuable. If reliable, NDVI could potentially be used to aid the study and conservation of a suite of taxa associated with difficult-to-access semi-arid regions of the Middle East and Central Asia, such as Asiatic Cheetah *Acinonyx jubatus venaticus* (IUCN Critically Endangered), Goitered Gazelle *Gazella subgutturosa* (IUCN Vulnerable), two subspecies of Asian Wild Ass *Equus hemionus onager* (IUCN Endangered) and *E. hemionus kulan* (Endangered) and Central Asian Tortoise *Testudo horsfieldii* (IUCN Vulnerable). Initial global analysis relating inter-annual NDVI to precipitation over 1982–1990 showed significant and positive correlation in semi-arid regions overall, but a non-significant correlation in most of Central Asia (Ichii et al., 2002). More recent studies of Central Asia, with greater sample size (spanning 1980s–2000s) showed a positive NDVI-rainfall correlation that, however, varied between land use/cover types (Nezlin et al., 2005; Propastin et al., 2008; Gessner et al., 2013). If both (a) the extent to which precipitation, as a proxy for potential vegetation productivity, explains observed NDVI and (b) the error or uncertainty in this signature can be related to landscape processes, this understanding of regional variation in NDVI-precipitation signature can assist the interpretation of NDVI and inform the scale at which it should be used (e.g. intra- or transregional). We expect that within arid to semi-arid areas those with relatively greater vegetation biomass (greater mean NDVI) will be more strongly (i.e. steeper regression slope) and clearly (greater R^2) responsive to precipitation, as there is more plant material to respond. Furthermore, vegetation degradation in areas of high livestock density may make NDVI less responsive to precipitation (provided livestock impacts are extensive relative to NDVI measurement grain) (Prince et al., 1998; Li et al., 2004).

To examine whether NDVI offers a potentially useful signal of vegetation productivity and semi-arid habitat structure across non-montane Central Asia, we examine its relationship with precipitation across the migratory range of a population of Asian Houbara *Chlamydotis macqueenii* (IUCN Vulnerable: BirdLife International, 2016) from the southern Kyzylkum Desert, Uzbekistan. Asian Houbara occupy vast and remote desert regions from the Middle East to China, and birds from Uzbekistan follow a similar migration as birds from East Kazakhstan along a “flyway” through Turkmenistan and around the Hindu Kush to wintering areas in southern Afghanistan, Pakistan, and Iran, where birds from China also winter (Combreau et al., 2011). NDVI could offer a proxy that may help understand constraints and settlement decisions on migration (routes and stopover sites), potential inter-annual variation in individual migration choices due to variations in rainfall, and carry-over effects of wintering site quality (Daunt et al., 2014; Rushing et al., 2016) on subsequent breeding productivity and survival. Across a large geographic area encompassing multiple ecoregions, we examine (1) the degree to which NDVI (from 2000–2015) relates to variation in precipitation (a) spatially (relating mean NDVI to mean precipitation, among degree cells); (b) inter-annually (within and across degree cells); (2) whether the NDVI-precipitation relation varies between ecoregions; and (3) possible drivers or correlates (mean NDVI and livestock density) of spatial variability in the strength of the NDVI-precipitation relation.

2. Methods

2.1 Study extent

We define our study extent as the outer borders (Fig 1a) of the migratory corridor and wintering range used by Asian Houbara that breed in Bukhara province, Uzbekistan, and migrate south to winter in Turkmenistan, Iran, Afghanistan and Pakistan (supported by 5 years of satellite telemetry data: Burnside et al., unpublished), together encompassing an area of 4.06 million km^2. Of the several desert and xeric shrubland World Wildlife Fund (WWF) terrestrial ecoregions (Olson et al., 2001) in our study area, we focus on five with varying shrub composition and density (Fig. 1b):

i) *Central Asian southern desert*, spanning the Karakum and Kyzylkum Deserts of Turkmenistan and Uzbekistan in the north of the study area, where seasonal precipitation is greatest during winter and spring;

ii) *Central Persian desert basins*, occupying western regions of central Iran and north-west Afghanistan, dominated by a large salt desert in the north and hot sand and gravel deserts in the east;

(iii) *South Iran Nubo-Sindian desert and semi-desert*, occupying a hilly coastal landscape bordering the north of the Persian Gulf on the southern and south-west limits of the study area;

(iv) *Registan-North Pakistan sandy desert*, lying east and south-east of the Central Persian desert basin, comprising semi-deserts in southern Afghanistan, sandy desert in Pakistan, and steppes in Iran; and

(v) *Baluchistan xeric woodlands*, lying further east in Pakistan and Afghanistan, with varied climate and topography.

2.2 Data processing

2.2.1 Constraints

We constrain the study window to 2000–2015 since higher-resolution Global Precipitation Climatology Project data are only available for this period. We constrain the study area by creating masks that exclude heavily modified anthropogenic land use/cover classes that do not support semi-arid, semi-natural shrub vegetation, and higher-elevation montane areas not used by Asian Houbara and expected to support different vegetation physiognomy. We derive land use/cover from Globcover 2009 data (Bontemps et al., 2011) with a 300 m spatial grain, and resample these to 1 km spatial grain using the nearest-neighbour algorithm, which assigns to each 1 km cell the classification of the nearest 300 m cell (Fig. 1a). We exclude from our land use/cover mask 1 km cells classified as irrigated, rain-fed and mosaic cropland where seasonal patterns of NDVI may be independent of precipitation. Globcover is reported to capture much of the extent of irrigated agriculture in Central Asia (Fritz et al., 2011), which we further confirmed by visual comparison with satellite imagery (S1-6). We found that Globcover underestimates the extent of mosaic and rain-fed agriculture (S7-14), so the higher vegetation productivity in these fields may introduce noise in the NDVI-precipitation relationship. We also exclude from our land use/cover mask at 1 km spatial grain artificial surfaces (i.e. urban areas), waterbodies and permanent snow and ice (Fig. 1a), as these also lack semi-arid vegetation and are unsuitable for houbara. Globcover misses some cities, waterbodies, and areas of ice and snow, again introducing noise in the NDVI-precipitation relationship, since NDVI in these areas is not expected to respond to rainfall (S15-34). However, given that excluded classes only make up ~16% (13% mosaic and rain-fed agriculture; all others < 3%) of the study area (compared to 7.6% cover by irrigated agriculture), their underestimation is unlikely to interfere substantially with the NDVI-precipitation relationship (S35). We map the land use/cover mask at 1 km spatial grain with all non-relevant classes excluded (S36). We produce an elevation layer by aggregating 90 m Shuttle Radar Tomography Mission (SRTM) data to 1 km spatial grain by computing the mean of all 90 m cells in each 1 km cell (S37a; Jarvis et al., 2015). We then examine the elevation of houbara migration, wintering, and breeding satellite-telemetry GPS fixes (excluding flight but including foraging movements, defined as those where mean speed between consecutive fixes is < 2 km hr^{-1}) for 61 wild birds tracked from 2011–2016 (see S37b for houbara fixes overlaid on elevation map), allowing us to exclude from our elevation mask at 1 km spatial grain cells above the 95th percentile of foraging elevations (1235 m) where houbara do not occur (see S37c for elevation mask).

2.2.2 NDVI

NDVI, the difference between the red (RED) and near infrared (NIR) spectral bands, expressed as (NIR – RED) / (NIR + RED), is positively associated with more green vegetation, as leaves absorb the photosynthetically active red band and reflect in the NIR; normalizing by the sum of the bands gives an index ranging from –1 to 1 (Tucker, 1979). We use Moderate Resolution Imaging Spectroradiometer (MODIS) NDVI, which has higher spatial resolution than other leading products (Pettorelli et al., 2005). For validation we use 1 km resolution data as smaller scales are not relevant to precipitation data; however, finer-grain MODIS NDVI (e.g. 250 m) would be relevant to fine-scale analysis of houbara movement. Monthly composites produce temporally-averaged, cloud-free NDVI images (NASA LP DAAC, 2015). We remove negative values, considered to represent unvegetated areas (e.g. saltpans, water, snow) (Huete et al., 1999), because NDVI will not respond to precipitation in these places. We average monthly 1 km spatial grain NDVI by year and map the mean across the years 2000–2015 (S38a). Additionally, we apply the 1 km spatial grain land use/cover and elevation masks to exclude areas where NDVI will not respond to precipitation and high-elevation areas where houbara are not found (S38b).

2.2.3 Precipitation

We quantify annual precipitation (mm.yr^{-1}) using the daily, 1 degree spatial grain Global Precipitation Climatology Project product (Huffman and Bolvin, 2013) (averaged by month from September 2000 to August 2015, see 2.2.4). This has global coverage at relatively high resolution, and is derived from both satellite and, importantly (as there are relatively few rain-gauges in the study area: Schneider et al., 2008), rain-gauge measurements (National Center for Atmospheric Research Staff, 2014). We aggregate the 1 km NDVI data to 1 degree spatial grain by computing the mean of all unmasked 1 km cells in each 1 degree cell, considering only those 1 degree cells with > 50 % of their area covered by unmasked 1 km cells. NDVI values of 1 degree cells retaining few 1 km cells after masking are likely to be biased because the small number of residual cells on the fringes of large masked regions of agriculture may be misclassified and also represent agriculture. Finally, we mask the 1 degree precipitation data by the masked 1 degree NDVI data so that their spatial extents are consistent and only suitable land uses/covers and elevations remain.

2.2.4 Summarizing annual NDVI and precipitation

Prior to analysis, preliminary data inspection revealed considerable geographic variation in seasonality across the study area, in terms of timing and length of periods of precipitation and NDVI (Fig. 2). As fixed growing and wet seasons could not be consistently defined, we calculate mean annual precipitation and NDVI. Annual mean NDVI is typically used to measure inter-annual variability in productivity and to determine how much of this variability is explained by annual average rainfall (Pettorelli et al., 2005). Although integrated NDVI can be calculated across year- and cell-specific 'growing seasons' defined by inflection points in the rate of change of monthly NDVI (Reed et al., 1994), this was not considered appropriate, given the low amplitude of annual NDVI variation and the erratic, ephemeral and sometimes unpredictable patterns of rainfall in the study region. We observe that the precipitation and NDVI signals are lowest in the summer months across all cells (Fig. 2; S39–44), but the timing of peak precipitation and vegetation growth varies geographically from autumn, through winter, to late winter/spring. To capture the majority of the precipitation and NDVI signals in a consistent one-year window, we measure both from the middle of summer in one year to the same in the next; thus autumn–winter–spring vegetation is related to precipitation from the same time-period. We tested different summer splits, and found the August–September split gave the best average fit of temporal models relating annual NDVI to precipitation in separate 1 degree cells (S45, see full temporal model description below). The fit of these models was not improved by offsetting precipitation and lagging NDVI by different numbers of months (assuming that NDVI signal follows precipitation) (S46); therefore we consider annual precipitation and annual NDVI from the beginning of September of year 1 to the end of August in year 2, aggregating autumnal, winter and spring rainfall and NDVI (15 annual intervals, from 2000 to 2015). We map the inter-annual mean and standard deviation of annual mean monthly NDVI and cumulative annual precipitation (Fig. 3), as well as the annual values of both variables (S47–48), which serve as inputs to models relating NDVI and precipitation across space and through time.

2.3 Relating NDVI to precipitation

2.3.1 Inter-annual mean (spatial relation)

To examine the spatial relation between long-term patterns of rainfall and NDVI, across replicate 1 degree cells (n=244) for the masked study area (see Fig. 3), we relate the inter-annual mean (across 2000–2015) of annual mean monthly NDVI (hereafter 'mean NDVI') to the inter-annual mean of cumulative annual precipitation ($mm.yr^{-1}$) (hereafter 'mean precipitation'), in a General Linear Model (GLM) fitted by least squares, with normal error and both variables log-transformed to satisfy homoscedasticity of model residuals. We do not consider temperature in the model or in the temporal analysis below (see 2.3.2) as precipitation has a greater influence on NDVI than temperature in semiarid regions globally (Ichii et al., 2002; Fensholt et al., 2012), and precipitation, but not temperature, correlates with growing season NDVI (March to November) in Central Asia (Propastin et al., 2008). We also examine whether this relation between mean NDVI and mean precipitation differs between ecoregions, testing the additive effect of ecoregion, the relation with mean precipitation and the interaction between these (different slope, response magnitude), assessed by a χ^2 test of -2 × (log likelihood ratio) of two nested models with degrees of freedom equal to the number of parameters removed.

2.3.2 By-cell annual mean (temporal variation)

Having explored the spatial association between mean (long-term) NDVI and rainfall, we then relate inter-annual variability (across 2000–2015, n= 15 years) in annual NDVI to cumulative annual precipitation ($mm.yr^{-1}$) (see S47–48 for model input layers). We examine the overall relation across the entire study area, using a Generalized Linear Mixed effects Model (GLMM, with normal error) incorporating precipitation as a fixed effect and random intercepts and slopes for each cell to control for pseudo-replication, conducted in lme4 (Bates et al., 2014). We again log-transform both variables to satisfy homoscedasticity and assess significance by a likelihood ratio test (tested as χ^2) on removing from the full model. Then, separately for each of the 244 1 degree cells in the area of interest, we relate annual NDVI to cumulative annual precipitation ($mm.yr^{-1}$) (both log-transformed), using independent general linear models. Mapped model results reveal spatial patterns in the effect size or strength (slope coefficient of NDVI-precipitation relation) and explanatory power (R^2) of the per degree cell models, which we then relate to covariates (mean NDVI, livestock density) to test *a priori* hypotheses (see 2.3.4).

2.3.3 Ecoregional variation

We expect spatial heterogeneity among semi-arid ecoregions in overall NDVI, precipitation and the information content of the NDVI-precipitation model. Variation in how responsive and tightly related (explanatory power) NDVI is to precipitation may signal that NDVI is a better proxy for habitat in some ecoregions than others, informing use of NDVI to examine winter site selection across the flyway, and whether it can be used at inter- as well as intra-regional scales. For the five semi-arid WWF ecoregions in the area of interest (Fig. 2b), we compare the inter-annual mean and standard deviation at 1 degree spatial grain of NDVI, mean and SD of cumulative precipitation ($mm.yr^{-1}$), and effect size (coefficient) and association strength (adjusted R^2) of per 1 degree cell NDVI-precipitation models, using a GLM with ecoregion as a categorical fixed effect (i.e. an ANOVA), comparing means between ecoregions by a Tukey HSD multiple comparison test conducted in the agricolae R package (Mendiburu, 2016).

2.3.4 Geographic correlates of NDVI-precipitation signature

We investigate factors that may explain spatial variation (among degree cells) in the strength of association (GLM slope and adjusted R^2) between NDVI and precipitation, considering inter-annual mean NDVI and livestock density as potential explanatory variables. Numbers of sheep and goats, the main livestock used in semi-arid areas and frequently blamed for vegetation degradation in the study area (Wint and Robinson, 2007), were summed from the Gridded Livestock of the World (GLW) dataset, aggregating from 0.05 degree to 1 degree resolution and log(1+x)-transforming to maintain homoscedasticity. As the variance inflation factor (VIF) of each of the two predictors was < 3 (S49), we consider that they are not collinear and can be simultaneously included in models (Zuur et al., 2010). We model the slope, and separately adj. R^2, as a linear function (GLM) of inter-annual mean NDVI and sheep and goat density km^{-2} at 1 degree spatial grain (n=244, see S50 for untransformed model input layers). In a separate GLM, relating slope of NDVI-precipitation to mean NDVI, we also examine differences (additive effects) of mean NDVI between ecoregions and the interaction of ecoregion and mean NDVI (does the strength of response of slope to mean NDVI differ between ecoregions). We expect steeper slopes in cells with greater vegetation density (inter-annual mean NDVI) and shallower slopes in lower density cells, however we would not expect the nature of this relationship to vary between ecoregions. For all models, we use backward elimination based on a χ^2 test of -2 × (log likelihood ratio) of two nested models with degrees of freedom equal to the number of parameters removed to assess parameter significance. The structure and specification of significant analytical models are summarized in Table 1.

3. Results

3.1 Relating NDVI to precipitation

Mean precipitation (2000–2015) at 1 degree spatial grain (n=244) over the Asian Houbara migratory range is highest (based on Tukey HSD test) in Baluchistan (455 $mm.yr^{-1}$ ± 182 sd), followed by Central Asia (337 ± 57.3), South Iran (289 ± 79.3), and Central Persia (273 ± 73.5), and lowest in Registan (195 ± 35.2) (Fig. 4a; S51). Following a similar pattern, mean NDVI (January–December) at 1 km spatial grain (n=2,863,519) is highest (based on Tukey HSD test) in Central Asia (0.125 $mm.yr^{-1}$ ± 0.0293 sd), and decreases in descending order in Baluchistan (0.119 ± 0.0485), South Iran (0.0942 ± 0.0385), Central Persia (0.0897 ± 0.0316) and Registan (0.0817 ± 0.0217) (Fig. 4b; S51).

Spatially, across the entire area of interest, long-term inter-annual mean NDVI (n= 15 years, 2000–2015) is greater in 1 degree cells (n=244) with higher long-term mean precipitation ($mm.yr^{-1}$) ($\chi^2_{(1)} = 15.02$, $p < 0.001$): NDVI = –5.98 $\pm$ 0.205 se + (0.654 $\pm$ 0.0353 se) × precipitation. Mean precipitation explained (adj. R^2) 58% of the variance in inter-annual mean NDVI per 1 degree cell. We show the NDVI-precipitation relationship by ecoregion (Fig. 5; Table 1, model 1), reducing the overall adj. R^2 to 0.48 because doing so limits the data extent (n=166, 1 degree cells). Incorporating a term for ecoregion (Table 1, model 2) improves model fit ($\chi^2_{(4)} = 2.04$, $p < 0.001$ on removal of ecoregion from the precipitation mean + ecoregion model), however the interaction between ecoregion and mean precipitation does not ($\chi^2_{(4)}$ = 0.14, p = 0.33 on removal of the interaction from the precipitation mean + ecoregion + ecoregion:precipitation mean model), indicating that the intercept but not the slope of the NDVI-precipitation relation differs among ecoregions. Compared to all other ecoregions, the intercept is significantly higher in Central Asia (controlling for table-wide significance with Holm adjustment, see S52-57 for full model results).

Temporally, across the area of interest (n=244, 1 degree cells) annual NDVI (n=15 across 2000–2015, n=3660 cell-year observations) was greater in years with higher cumulative annual precipitation (mm.yr^{-1}); in a GLMM controlling for degree cell (random intercepts and slopes; Table 1, model 3) ($\chi^2_{(1)}$ = 314.15, p < 0.001, Marginal R^2_{GLMM} = 0.14, Conditional R^2_{GLMM} = 0.95): NDVI = –3.6 $\pm$ 0.044 se + (0.23 $\pm$ 0.0091 se) × precipitation. Separate general linear models (with normal error) relating annual NDVI to cumulative annual precipitation for each of the 244 1 degree cells, had a similar mean slope (0.233 $\pm$ 0.157 sd) and a mean adj. R^2 of 0.436 $\pm$ 0.231 sd (Table 1, model 4; Fig. 6), confirming the strong overall temporal relation but revealing considerable spatial variation in its strength and explanatory power.

3.2 Geographic correlates of NDVI-precipitation signature

NDVI-precipitation model results systematically differed between the five semi-arid WWF ecoregions. Slope values of the 244 separate 1 degree cell linear models relating mean annual NDVI to cumulative annual precipitation (mm.yr^{-1}) are two or more times greater (based on Tukey HSD test) in Central Asia (0.291 ± 0.154 sd), Baluchistan (0.2330 ± 0.107) and South Iran (0.199 ± 0.0910) than in Registan (0.105 ± 0.0553) and Central Persia (0.0707 ± 0.0763), which are similar (Fig. 7a; S51). Adjusted R^2 values (n=244) of separate 1 degree cell linear models are higher (based on Tukey HSD test) in Baluchistan (0.627 ± 0.117 sd), Registan (0.553 ± 0.176) and South Iran (0.544 ± 0.201) than in Central Asia (0.476 ± 0.177), and are more than three times higher in these first three regions than in Central Persia (0.166 ± 0.176) (Fig. 7b; S51). Mean NDVI and livestock density in part explain this heterogeneity in NDVI-precipitation relation. The strength (slope coefficient) of the NDVI-precipitation relation per 1 degree cell, is greater in cells with greater mean NDVI (Table 1, model 5) ($\chi^2_{(1)}$ = 2.26, p < 0.001, adj. R^2 = 0.38): slope = –0.0624 $\pm$ 0.0259 se + (2.5 $\pm$ 0.207 se) × mean NDVI, but was not affected by livestock density ($\chi^2_{(1)}$ = 0.04, p = 0.099 on removing livestock from model including mean NDVI). In contrast, the explanatory power (adjusted R^2) of per 1 degree cell NDVI-precipitation models is weakly, but positively, related to livestock density (Table 1, model 6) ($\chi^2_{(1)}$ = 0.33, p = 0.0105, adj. R^2 = 0.023): adj. R^2 = 0.403 $\pm$ 0.0202 se + (0.0203 $\pm$ 0.00793 se) × livestock density, but not to mean NDVI ($\chi^2_{(1)}$ = 0.03, p = 0.416 on removing mean NDVI from model including livestock). In the separate models testing ecoregion influence on the slope of the NDVI-precipitation relation (Table 1, model 7), ecoregion is significant ($\chi^2_{(4)}$ = 0.41, p < 0.001 on removing ecoregion from the NDVI mean + ecoregion model), however the interaction of ecoregion and mean NDVI is not ($\chi^2_{(4)}$ = 0.04, p = 0.46 on removing the interaction from the NDVI mean + ecoregion + ecoregion:NDVI mean model), indicating that the intercept but not the slope of the relation varies between ecoregions. Pairwise comparison shows significant groupings between ecoregions (controlling for table-wide significance with holm adjustment, see S58-65 for full model results).

4. Discussion

4.1 NDVI as a vegetation proxy

Overall, MODIS NDVI is positively related to precipitation and thus offers information on spatial and temporal variation in green vegetation biomass across the Asian Houbara's range. The significance and high explanatory power of models relating per 1 degree cell mean NDVI to mean precipitation indicates a strong geographic relation between regional rainfall levels and vegetation biomass across this wide sweep of arid and semi-arid ecosystems. Areas with greater mean rainfall (such as the southern Central Asian desert and Baluchistan xeric woodlands) had greater mean NDVI. Furthermore, both within and across ecoregions, temporal (inter-annual) variation in annual NDVI was strongly and significantly related to variation in annual precipitation, supporting the interpretation of NDVI as providing information on local temporal variation in vegetation cover and productivity. Importantly, the response of annual NDVI to annual precipitation varied among ecoregions and at finer (1 degree) scales, with the strength (slope) of this signature positively related to mean NDVI. This is not surprising, as areas that have greater vegetation biomass and thus NDVI have more vegetation available to respond (in terms of contributing to the NDVI increment) to a given change in precipitation volume and thus water availability. This suggests that semi-arid landscapes with greater long-term levels of vegetation cover may experience greater amplitude of temporal variability in habitat quality for a given amplitude of climatic variation. It is surprising, therefore, that the strength of association (R^2) between annual NDVI and annual precipitation was not also related to mean NDVI. However, other differences in vegetation structure and plant species composition (or temperature) between ecoregions may also affect the slope of the NDVI-precipitation relation; South Iran has mean NDVI that is broadly similar to (though significantly greater than) that of Central Persia and Registan, but is almost twice as sensitive to precipitation.

Unexpectedly, the robustness of the temporal NDVI-precipitation relation (in terms of the adj. R^2 of temporal per-cell models) increases rather than decreases with livestock density. It may be that the coarse spatial grain of the analysis, which resamples Gridded Livestock of the World data from a 0.05 to 1 degree spatial grain, obscures a finer-scale negative relationship that has been found between NDVI and livestock, e.g. at scales of one or a few kilometers relative to settlement foci or watering points (Behnke et al., 2006; Rajabov et al., 2009). At the coarse scale of our analysis, as constrained by resolution of precipitation data, it is likely that more livestock are grazed where there is more green vegetation. However, the positive association between NDVI-precipitation adj. R^2 and livestock density suggests that widely assumed perceptions of widespread degradation by livestock (e.g. MEA), sometimes socially constructed without objective evidence (e.g. Stringer, 2008), may not be reflected in landscape-scale measures of vegetation. Notably, Koshkin et al. (2014) found no evidence that extensive livestock browsing in Bukhara province, Uzbekistan, altered semi-arid shrub vegetation structure at landscape scales. Though by showing NDVI relates to rainfall, and is thus a robust measure of vegetation volume, we validate its use (at appropriate scales) to further explore degradation effects at finer resolutions.

4.2 Implications for species habitat modelling

The broad spatial and temporal association between mean and annual NDVI and precipitation, across the full extent of the area of interest (spanning five WWF arid or semi-arid ecoregions), suggests that NDVI could be used as a proxy for vegetation abundance through space and time even at such wide geographic scales. Demographic data for Asian Houbara may support this. Breeding population densities are an order of magnitude higher in the Kyzylkum Desert (within Central Asian ecoregion; 0.06 birds per square km) than in northern Iran (within Central Persian ecoregion; 0.008 birds per square km: Allinson, 2014), where mean NDVI are 0.1250 and 0.0897 respectively, although intensity of local persecution may be an additional factor (Goriup, 1997).

Owing to limitations in availability of precipitation data we conducted our analysis at a spatial grain of 1 degree, while ecological analyses in relation to bird or animal movements, and analyses examining demographic responses to habitat quality at wintering sites, will likely be conducted at finer spatial grain. Nevertheless, we expect that the spatial and temporal NDVI-precipitation relation would be robust at such finer scales, as the relation detected at coarse scales is a summation of the localized responses of vegetation to prevailing precipitation. Furthermore, as the coarse-grain resolution of precipitation data averages across rainfall events that may be localized and spatially variable within arid regions (Noy-Meir, 1973), the vegetation response may be even stronger at local scales if suitable fine-grain precipitation data are available for such analysis. Lastly, resampling (averaging) NDVI across degree cells removes ecologically important information relating to localized topography (e.g. wadis and salt pans or solonchaks) and localized habitat degradation (e.g. in close proximity to villages or wells: Behnke et al., 2006; Rajabov et al., 2009), potentially making finer-scale NDVI more informative.

As annual NDVI was responsive to temporal variation in annual precipitation, for a given wintering area NDVI (or NDVI anomaly relative to the local inter-annual mean) can be used as a proxy for temporal variation in habitat quality to examine potential carry-over effects between years for individuals wintering within the same ecoregion. NDVI also offers the potential to examine stopover and wintering site selection relative to other available areas within the same ecoregional landscapes, potentially reflecting local variation in plant community composition, structure and productivity (e.g. through substrate and topography) but also habitat degradation.

At greater study scales across the flyway, it appears appropriate to use mean inter-annual NDVI as a proxy for relative habitat quality or vegetation productivity between and across ecoregions that differ in bioclimatic character, owing to the broad spatial correlation between mean NDVI and mean precipitation and the overall positive relation between the strength of the temporal NDVI-precipitation signature and per-cell mean NDVI. However, when examining site selection and inter-annual carry-over effects (i.e. by relating subsequent performance to inter-annual variation in habitat quality at a location) simultaneously across individuals wintering in different ecoregions (i.e. to maximize sample size); variation in the strength of the NDVI-precipitation signature advises caution. Central Asia has greater NDVI for the same level of precipitation than all other ecoregions (significant additive effect), however ecoregion does not influence how much mean NDVI increases for a given precipitation increment (non-significant interaction), suggesting comparison of site selection effects is appropriate across wintering ecoregions (Central Persia, Registan, South Iran, and Baluchistan) but should be considered separately for breeding (Central Asia, versus other ecoregions). Similarly, the slope of the relation between annual NDVI and annual precipitation differs for the same mean NDVI by ecoregion (significant additive effect), but ecoregion does not affect how much the slope increases for a given mean NDVI increment (non-significant interaction), supporting comparison of carry-over effects only between ecoregions. Validating NDVI across space and time in arid and semi-arid environments opens the way to understanding how it relates to species' habitat, which will aid in the study and conservation of the Asian Houbara and other threatened species which share its range.

Acknowledgements

We thank two anonymous reviewers for their helpful comments on an earlier version of the manuscript. A. F. Formica and R. J. Burnside were funded by the Ahmed bin Zayed Charitable Foundation.

References

Allinson, T. 2014. Review of the global conservation status of the Asian Houbara Bustard *Chlamydotis macqueenii*. Report to the Convention on Migratory Species Office – Abu Dhabi. BirdLife International, Cambridge.

Bates, D., Mächler, M., Bolker, B., Walker, S., 2014. Fitting linear mixed-effects models using lme4. Submitt. to J. Stat. Softw. 67, 51. doi:10.18637/jss.v067.i01

Behnke, R., Davidson, G., Jabbar, A., Coughenour, M., 2008. Human and natural factors that influence livestock distributions and rangeland desertification in Turkmenistan, in: Behnke, R. (Ed.), The Socio-Economic Causes and Consequences of Desertification in Central Asia. Springer Netherlands, Dordrecht, pp. 141–168. doi:10.1007/978-1-4020-8544-4_7

BirdLife International, 2016. Species factsheet: *Chlamydotis macqueenii* [WWW Document]. URL http://datazone.birdlife.org/species/factsheet/22733562

Bontemps, S., Defourny, P., Bogaert, E. Van, Kalogirou, V., Perez, J.R., 2011. GLOBCOVER 2009 products description and validation report. ESA Bull. doi:10013/epic.39884.d016

Bridge, E.S., Ross, J.D., Contina, A.J., Kelly, J.F., 2016. Do molt-migrant songbirds optimize migration routes based on primary productivity? Behav. Ecol. 27, 784–792. doi:10.1093/beheco/arv199

Combreau, O., Riou, S., Judas, J., Lawrence, M., Launay, F., 2011. Migratory pathways and connectivity in Asian Houbara bustards: Evidence from 15 years of satellite tracking. PLoS One 6. doi:10.1371/journal.pone.0020570

Daunt, F., Reed, T.E., Newell, M., Burthe, S., Phillips, R.A., Lewis, S., Wanless, S., 2014. Longitudinal bio-logging reveals interplay between extrinsic and intrinsic carry-over effects in a long-lived vertebrate. Ecology 95, 2077–2083. doi:10.1890/13-1797.1

de Mendiburu, F., 2016. agricolae: Statistical procedures for agricultural research [WWW Document]. URL https://cran.r-project.org/package=agricolae

Fensholt, R., Langanke, T., Rasmussen, K., Reenberg, A., Prince, S.D., Tucker, C., Scholes, R.J., Le, Q.B., Bondeau, A., Eastman, R., Epstein, H., Gaughan, A.E., Hellden, U., Mbow, C., Olsson, L., Paruelo, J., Schweitzer, C., Seaquist, J., Wessels, K., 2012. Greenness in semi-arid areas across the globe 1981-2007 - an Earth Observing Satellite based analysis of trends and drivers. Remote Sens. Environ. 121, 144–158. doi:10.1016/j.rse.2012.01.017

Fritz, S., See, L., McCallum, I., Schill, C., Obersteiner, M., van der Velde, M., Boettcher, H., Havlík, P., Achard, F., 2011. Highlighting continued uncertainty in global land cover maps for the user community. Environ. Res. Lett. 6, 44005. doi:10.1088/1748-9326/6/4/044005

Gamon, J.A., Field, C.B., Goulden, M.L., Griffin, K.L., Hartley, A.E., Joel, G., Penuelas, J., Valentini, R., 1995. Relationships between NDVI, canopy structure, and photosynthesis in three Californian vegetation types. Ecol. Appl. 5, 28–41. doi:10.2307/1942049

Gessner, U., Naeimi, V., Klein, I., Kuenzer, C., Klein, D., Dech, S., 2013. The relationship between precipitation anomalies and satellite-derived vegetation activity in Central Asia. Glob. Planet. Change 110, 74–87. doi:10.1016/j.gloplacha.2012.09.007

Goriup, P.D., 1997. The world status of the Houbara bustard *Chlamydotis undulata*. Bird Conserv. Int. 7, 373–397. doi:10.1017/S0959270900001714

Grande, J.M., Serrano, D., Tavecchia, G., Carrete, M., Ceballos, O., Díaz-Delgado, R., Tella, J.L., Donázar, J.A., 2009. Survival in a long-lived territorial migrant: Effects of life-history traits and ecological conditions in wintering and breeding areas. Oikos 118, 580–590. doi:10.1111/j.1600-0706.2009.17218.x

Hu, J., Jiang, Z., 2011. Climate change hastens the conservation urgency of an endangered ungulate. PLoS One 6. doi:10.1371/journal.pone.0022873

Huete, A.R., Jackson, R.D., 1985. Spectral response of a plant canopy with different soil backgrounds. Remote Sens. Environ. 17, 37–53. doi:Doi 10.1016/0034-4257(85)90111-7

Huffman, G., Bolvin, D., 2013. Version 1.2 GPCP one-degree daily precipitation data set documentation [WWW Document]. doi:http://dx.doi.org/10.5065/D6D50K46. Accessed 24 May 2016

Ichii, K., Kawabata, a., Yamaguchi, Y., 2002. Global correlation analysis for NDVI and climatic variables and NDVI trends: 1982-1990. Int. J. Remote Sens. 23, 3873–3878. doi:10.1080/01431160110119416

Jarvis, A., H.I., Reuter, A., Nelson, A., Guevara, E., 2016. Hole-filled SRTM for the globe Version 4, available from the CGIAR-CSI SRTM 90m Database [WWW Document]. CGIAR CSI Consort. Spat. Inf. doi:http://srtm.csi.cgiar.org

Kaufman, Y.J., Tanré, D., Markham, B., Gitelson, A.A., 1992. Atmospheric effects on the NDVI-strategies for its removal. Int. Sp. Year Sp. Remote Sensing, Vols 1 2 1238–1241. doi:10.1109/IGARSS.1992.578402.

Li, J., Lewis, J., Rowland, J., Tappan, G., Tieszen, L.L., 2004. Evaluation of land performance in Senegal using multi-temporal NDVI and rainfall series. J. Arid Environ. 59, 463–480. doi:10.1016/j.jaridenv.2004.03.019

Millennium Ecosystem Assessment, 2005. Ecosystems and human well-being: desertification synthesis, in: Ecosystems and human well-being. World Resources Institute, Washington, DC., p. 26. doi:ISBN: 1-56973-590-5

NASA LP DAAC, 2015. MOD13A3: MODIS/Terra vegetation indices monthly L3 global 1km V005 [WWW Document]. URL https://lpdaac.usgs.gov/dataset_discovery/modis/modis_products_table/mod13a3

National Center for Atmospheric Research Staff, 2014. The climate data guide: precipitation data sets: overview & comparison table [WWW Document]. URL https://climatedataguide.ucar.edu/climate-data/precipitation-data-sets-overview-comparison-table

Nezlin, N.P., Kostianoy, A.G., Li, B.L., 2005. Inter-annual variability and interaction of remote-sensed vegetation index and atmospheric precipitation in the Aral Sea region. J. Arid Environ. 62, 677–700. doi:10.1016/j.jaridenv.2005.01.015

Noy-Meir, I., 1973. Desert ecosystems: environment and producers. Annu. Rev. Ecol. Stystematics 4, 25–51. doi:10.1146/annurev.es.04.110173.000325

Olson, D.M., Dinerstein, E., Wikramanayake, E.D., Burgess, N.D., Powell, G.V.N., Underwood, E.C., D'amico, J. a., Itoua, I., Strand, H.E., Morrison, J.C., Loucks, C.J., Allnutt, T.F., Ricketts, T.H., Kura, Y., Lamoreux, J.F., Wettengel, W.W., Hedao, P., Kassem, K.R., 2001. Terrestrial ecoregions of the world: a new map of life on earth. Bioscience 51, 933. doi:10.1641/0006-3568(2001)051[0933:TEOTWA]2.0.CO;2

Parra, J.L., Graham, C.C., Freile, J.F., 2004. Evaluating alternative data sets for ecological niche models of birds in the Andes. Ecography (Cop.). 27, 350–360. doi:10.1111/j.0906-7590.2004.03822.x

Pettorelli, N., Gaillard, J.M., Mysterud, A., Duncan, P., Stenseth, N.C., Delorme, D., Van Laere, G., Toïgo, C., Klein, F., 2006. Using a proxy of plant productivity (NDVI) to find key periods for animal performance: The case of roe deer. Oikos 112, 565–572. doi:10.1111/j.0030-1299.2006.14447.x

Pettorelli, N., Ryan, S., Mueller, T., Bunnefeld, N., Jedrzejewska, B., Lima, M., Kausrud, K., 2011. The Normalized Difference Vegetation Index (NDVI): Unforeseen successes in animal ecology. Clim. Res. 46, 15–27. doi:10.3354/cr00936

Pettorelli, N., Vik, J.O., Mysterud, A., Gaillard, J.M., Tucker, C.J., Stenseth, N.C., 2005. Using the satellite-derived NDVI to assess ecological responses to environmental change. Trends Ecol. Evol. 20, 503–510. doi:10.1016/j.tree.2005.05.011

Prince, S.D., Brown De Colstoun, E., Kravitz, L.L., 1998. Evidence from rain-use efficiencies does not indicate extensive Sahelian desertification. Glob. Chang. Biol. 4, 359–374. doi:10.1046/j.1365-2486.1998.00158.x

Propastin, P.A., Kappas, M., Muratova, N.R., 2008. Inter-annual changes in vegetation activities and their relationship to temperature and precipitation in Central Asia from 1982 to 2003. J. Environ. Informatics 12, 75–87. doi:10.3808/jei.200800126

Rajabov, T., 2009. Ecological assessment of spatio-temporal changes of vegetation in response to piosphere effects in semi-arid rangelands of Uzbekistan [WWW Document]. URL http://www.unulrt.is/static/fellows/document/rajabov-t.pdf

Reed, B.C., Brown, J.F., VanderZee, D., Loveland, T.R., Merchant, J.W., Ohlen, D.O., 1994. Measuring phenological variability from satellite imagery. J. Veg. Sci. 5, 703–714. doi:10.2307/3235884

Rushing, C.S., Marra, P.P., Dudash, M.R., 2016. Winter habitat quality but not long-distance dispersal influences apparent reproductive success in a migratory bird. Ecology 97, 1218–1227. doi:10.1890/15-1259.1/suppinfo

Saino, N., Szép, T., Romano, M., Rubolini, D., Spina, F., Møller, A.P., 2004. Ecological conditions during winter predict arrival date at the breeding quarters in a trans-Saharan migratory bird. Ecol. Lett. 7, 21–25. doi:10.1046/j.1461-0248.2003.00553.x

Saino, N., Szép, T., Romano, M., Rubolini, D., Spina, F., Møller, A.P., 2004. Ecological conditions during winter predict arrival date at the breeding quarters in a trans-Saharan migratory bird. Ecol. Lett. 7, 21–25. doi:10.1046/j.1461-0248.2003.00553.x

Schaub, M., Kania, W., Köppen, U., 2005. Variation of primary production during winter induces synchrony in survival rates in migratory white storks *Ciconia ciconia*. J. Anim. Ecol. 74, 656–666. doi:10.1111/j.1365-2656.2005.00961.x

Schneider, U., Becker, A., Ziese, M., Rudolf, B., 2011. Global Precipitation Analysis Products of the GPCC [WWW Document]. doi:10.5676/DWD_GPCC/MP_M_V5_100

Singh, N.J., Milner-Gulland, E.J., 2011. Conserving a moving target: Planning protection for a migratory species as its distribution changes. J. Appl. Ecol. 48, 35–46. doi:10.1111/j.1365-2664.2010.01905.x

Stringer, L.C., 2008. From Global environmental discourse to local adaptations and responses: a desertification research agenda for Central Asia, in: Behnke, R. (Ed.), The socio-economic causes and consequences of desertification in Central Asia. Springer Netherlands, Dordrecht, pp. 13–31. doi:10.1007/978-1-4020-8544-4_2

Tøttrup, A.P., Thorup, K., Rainio, K., Yosef, R., Lehikoinen, E., Rahbek, C., 2008. Avian migrants adjust migration in response to environmental conditions en route. Biol. Lett. 4, 685–688. doi:10.1098/rsbl.2008.0290

Tucker, C.J., Sellers, P.J., 1986. Satellite remote-sensing of primary production. Int. J. Remote Sens. 7, 1395–1416.

Tucker, C.J., 1979. Red and photographic infrared linear combinations for monitoring vegetation. Remote Sens. Environ. 8, 127–150. doi:10.1016/0034-4257(79)90013-0

Weiss, J.L., Gutzler, D.S., Coonrod, J.E.A., Dahm, C.N., 2004. Long-term vegetation monitoring with NDVI in a diverse semi-arid setting, central New Mexico, USA. J. Arid Environ. 58, 249–272. doi:10.1016/j.jaridenv.2003.07.001

Wint, W., Robinson, R., 2007. Gridded Livestock of the World [WWW Document]. Organization. doi:10.1017/CBO9781107415324.004

Yang, Y., Long, D., Guan, H., Scanlon, B.R., Simmons, C.T., Jiang, L., Xu, X., 2014. GRACE satellite observed hydrological controls on interannual and seasonal variability in surface greenness over mainland Australia. J. Geophys. Res. G Biogeosciences 119, 2245–2260. doi:10.1002/2014JG002670

Zuur, A.F., Ieno, E.N., Elphick, C.S., 2010. A protocol for data exploration to avoid common statistical problems. Methods Ecol. Evol. 1, 3–14. doi:10.1111/j.2041-210X.2009.00001.x

Figure legends

Figure 1. Maps of (a) land use/cover (Bontemps et al., 2011) and (b) elevation (Jarvis et al., 2015) overlaid with semi-arid WWF ecoregions (Olson et al., 2001) at 1 km spatial grain. See supplementary information for validation of mapped land use/cover data with Google Earth imagery.

Figure 2. Mean monthly precipitation ($mm.month^{-1}$) and NDVI (mean per month, across 2000–2014, late 2015 data unavailable) for degree cells sampled within each of five semi-arid ecoregions. The month axis is offset from minimum to minimum. For reference are a vertical red line at March and gray box from February to May.

Figure 3. Inter-annual mean and standard deviation of mean annual NDVI (a, b) and cumulative annual precipitation ($mm.yr^{-1}$) (c, d) across 2000–2015 at 1 degree spatial grain masked by land use/cover and elevation.

Figure 4. Box and whisker plots for each semi-arid ecoregion of the inter-annual mean of (a) cumulative annual precipitation ($mm.yr^{-1}$) and (b) mean annual NDVI across 2000–2015, at 1 km and 1 degree spatial grain. Plots show the median, boxes bound the second and third quartiles, lower and upper whiskers extend to the most distal value within 1.5 × IQR (inter-quartile range) of the second and third quartiles respectively, with outliers beyond the whiskers plotted as points. Superscripts show homogenous subsets identified by Tukey HSD tests.

Figure 5. Inter-annual mean of mean annual NDVI versus cumulative annual precipitation ($mm.yr^{-1}$) at 1 degree spatial grain (n=244) for the extent of the five ecoregions and by individual ecoregion across 2000–2015. NDVI significantly relates to precipitation ($\chi^2_{(1)}$ = 15.02, $p < 0.001$, adj. $R^2 = 0.58$): NDVI = –5.98 $\pm$ 0.205 se + (0.654 $\pm$ 0.0353 se) × precipitation across the full area of interest. However showing the relationship by ecoregion limits the data extent, reducing the overall adj. R^2 to 0.48.

Figure 6. Slope (a) and adjusted R^2 (b) separately for each of 244 1 degree cells in the area of interest, of GLMs (with normal error) relating annual NDVI to cumulative annual precipitation ($mm.yr^{-1}$) across 2000–2015 (n=15). We map the slope and adj. R^2 for log-transformed data (to satisfy homoscedasticity) of models across cells. Mean slope and R^2 across cells are 0.233 $\pm$ 0.157 sd and 0.436 $\pm$ 0.231 sd.

Figure 7. Box and whisker plots for each semi-arid ecoregion of the (a) slope and (b) adjusted R^2 values of the 244 separate 1 degree cell linear models relating mean annual NDVI to cumulative annual precipitation ($mm.yr^{-1}$) (2000–2015, n=244). Plots show the median, boxes bound the second and third quartiles, lower and upper whiskers extend to

the most distal value within 1.5 × IQR (inter-quartile range) of the second and third quartiles respectively with outliers beyond the whiskers plotted as points.

Figures

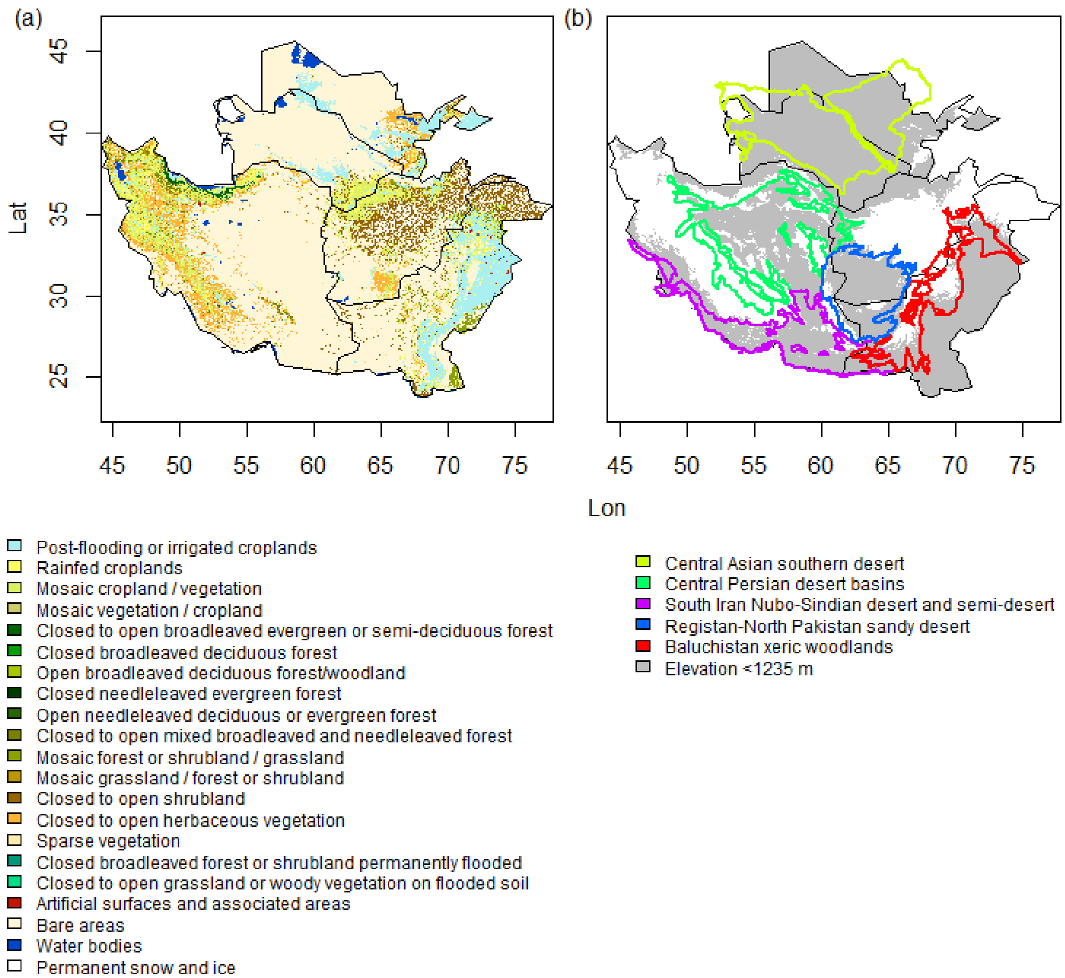

Figure 1.

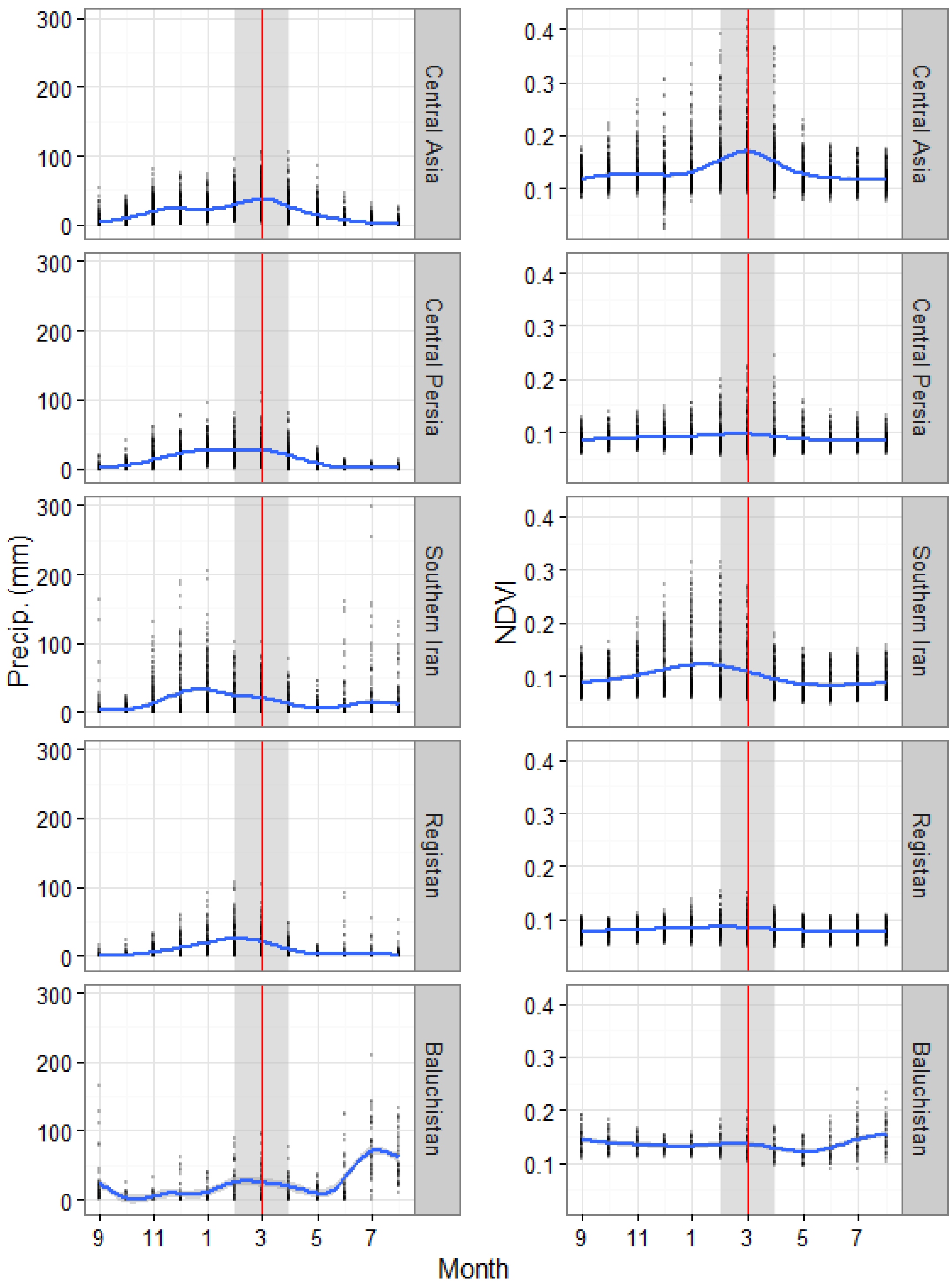
Precip. (mm)
NDVI
Month
Central Asia
Central Persia
Southern Iran
Registan
Baluchistan
0
100
200
300
0.1
0.2
0.3
0.4
9
11
1
3
5
7

Figure 2.

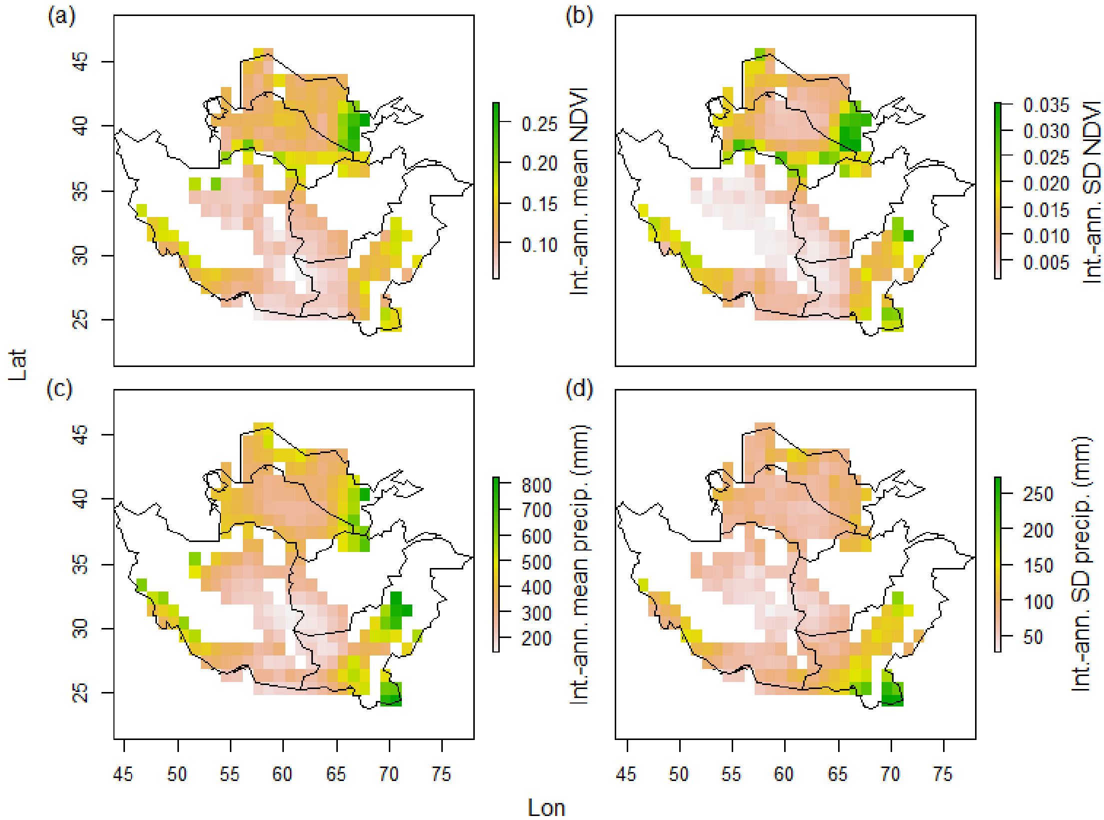

Figure 3.

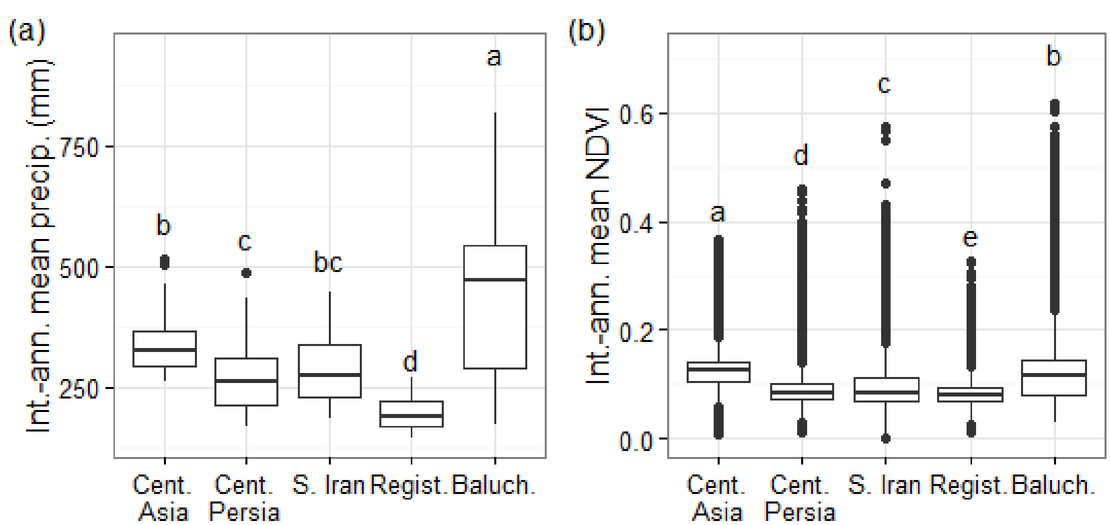

Figure 4.

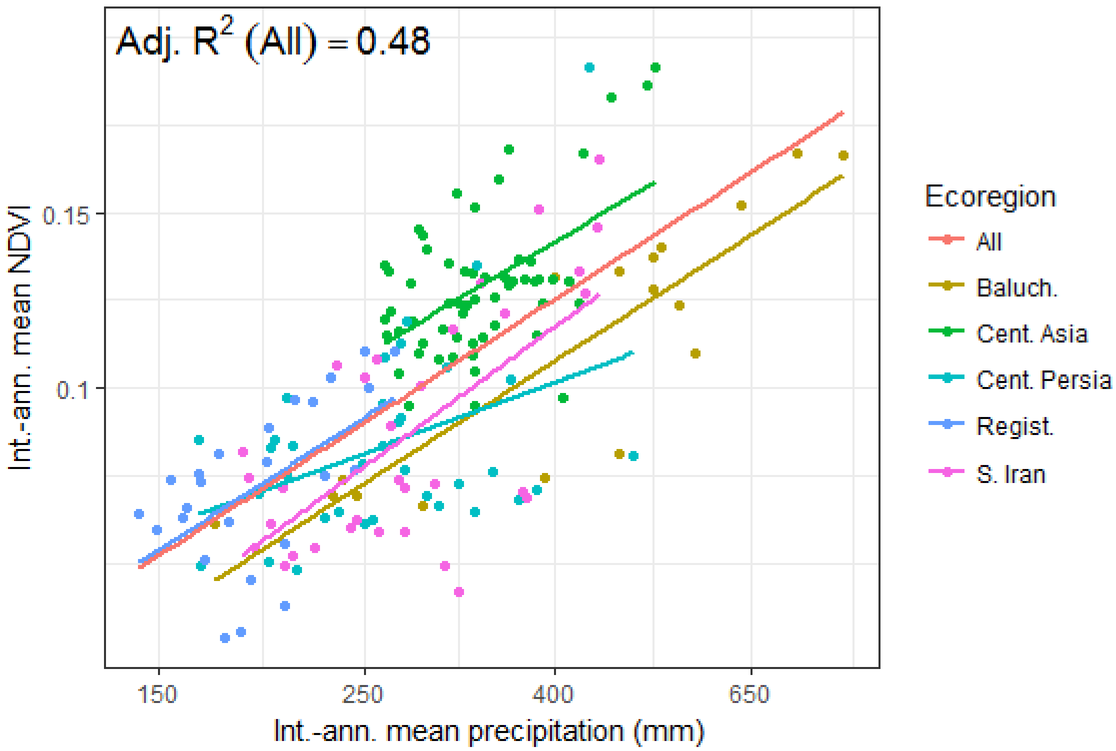

Adj. R^2 (All) = 0.48
Int.-ann. mean NDVI
0.15
0.1
150
250
400
650
Int.-ann. mean precipitation (mm)
Ecoregion
All
Baluch.
Cent. Asia
Cent. Persia
Regist.
S. Iran

Figure 5.

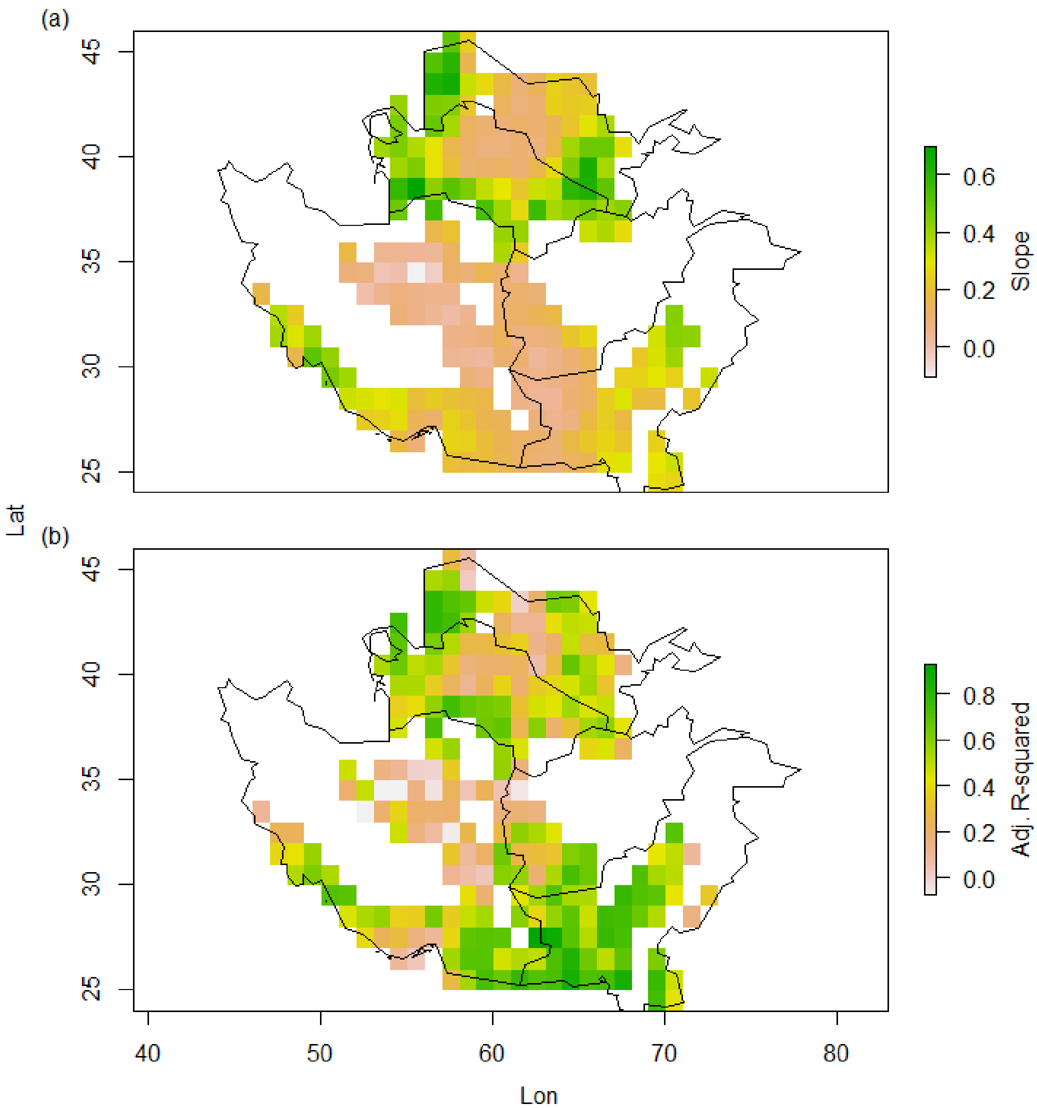
(a)
(b)
Lat
Lon
Slope
Adj. R-squared
45
40
35
30
25
40
50
60
70
80
0.0
0.2
0.4
0.6
0.8

Figure 6.

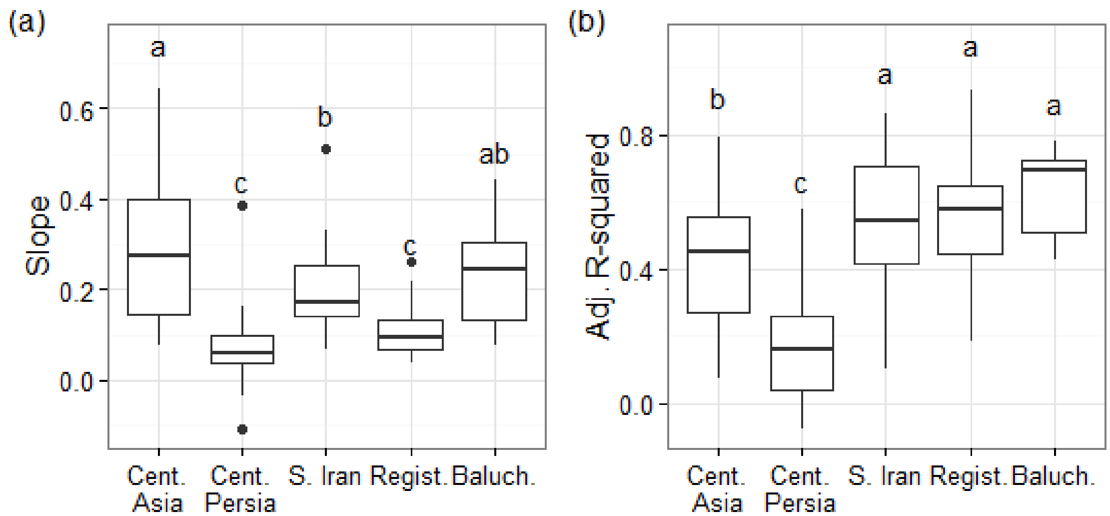
(a)
Slope
0.6
0.4
0.2
0.0
a
c
b
c
ab
Cent. Asia
Cent. Persia
S. Iran
Regist.
Baluch.
(b)
Adj. R-squared
0.8
0.4
0.0
b
c
a
a
a
Cent. Asia
Cent. Persia
S. Iran
Regist.
Baluch.

Figure 7.

Tables

Table 1. Summary of models analyzed, specifying model structure, response and predictor variables, overall model significance and explanatory power. GLM denotes a General Linear Model, GLMM a Generalised Linear Mixed effects Model, for which M-R^2_{GLMM} is the Marginal R^2, and C-R^2_{GLMM} the Conditional R^2. χ^2 tests the change in model performance relative to the null model, or on model simplification (removal of ecoregion term, models 2 and 7).

Model	Response	Predictor(s)	Structure	n cells	χ^2	p	R^2
1	Inter-annual mean NDVI	Inter-annual mean precipitation ($mm.yr^{-1}$)	GLM (across cells)	166	$\chi^2_{(1)}$ = 6.47	<0.001	adj. R^2 = 0.48
2	Inter-annual mean NDVI	Inter-annual mean precipitation ($mm.yr^{-1}$), ecoregion	GLM (across cells)	166	$\chi^2_{(4)}$ = 2.04	<0.001	adj. R^2 = 0.62
3	Annual NDVI	Annual precipitation ($mm.yr^{-1}$), Cell ID (random)	GLMM (across cells)	3660 cell-year observations	$\chi^2_{(1)}$ = 314.15	<0.001	M-R^2_{GLMM} = 0.14, C-R^2_{GLMM} = 0.95
4	Annual NDVI	Annual precipitation ($mm.yr^{-1}$)	GLM (per cell)	244			Mean adj. R^2 = 0.436 $\pm$ 0.231 sd
5	Annual NDVI-precipitation slope per cell (β of model 4)	Inter-annual mean NDVI	GLM (across cells)	244	$\chi^2_{(1)}$ = 2.26	<0.001	adj. R^2 = 0.38
6	Annual NDVI-precipitation adj. R^2 per cell (of model 4)	Livestock density	GLM (across cells)	244	$\chi^2_{(1)}$ = 0.33	0.0105	adj. R^2 = 0.023
7	Annual NDVI-precipitation slope per cell (β of model 4)	Inter-annual mean NDVI, ecoregion	GLM (across cells)	166	$\chi^2_{(4)}$ = 0.41	<0.001	adj. R^2 = 0.50

Supplementary information

Side-by-side comparisons of Globcover 2009 classification and Google Earth satellite imagery.

Cropland

Large areas of continuous cropland

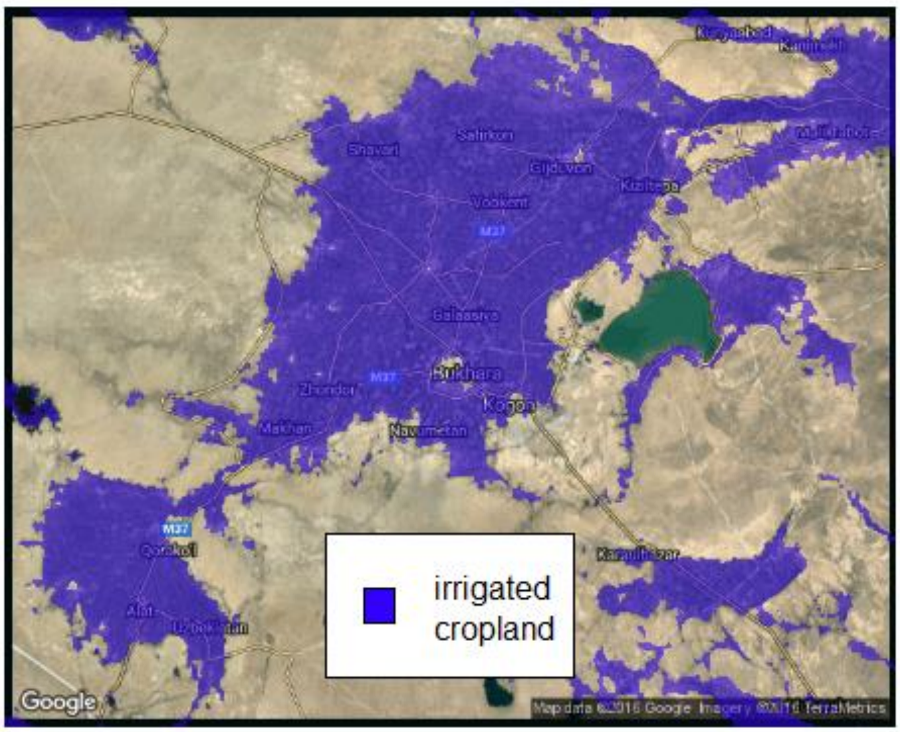

S1: Irrigated cropland in Bukhara, Uzbekistan

S2: Satellite view of Bukhara, Uzbekistan

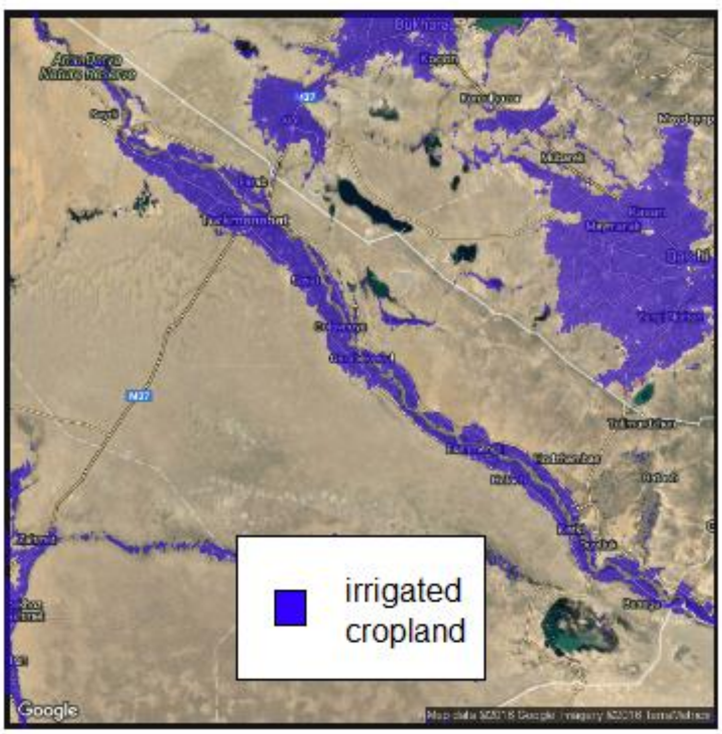

S3: Irrigated cropland along the Amu Darya near the Uzbekistan–Turkmenistan border

S4: Satellite view of the Amu Darya near the Uzbekistan–Turkmenistan border

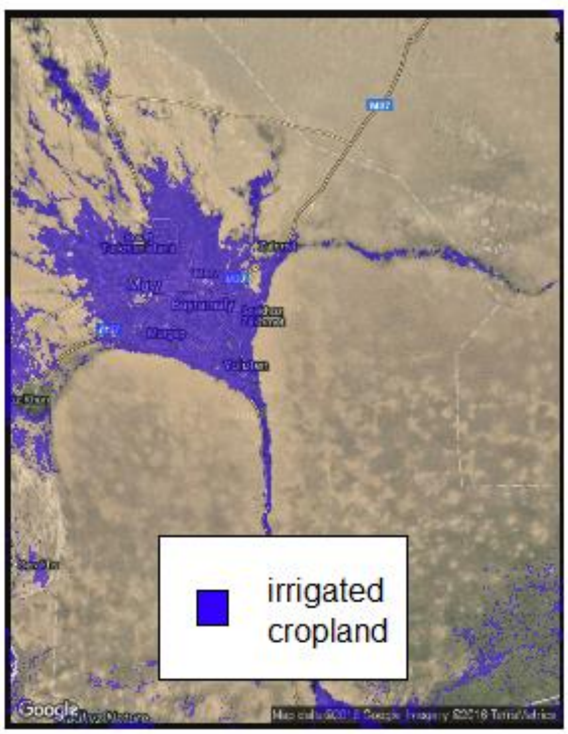

S5: Irrigated cropland in Mary, Turkmenistan

S6: Satellite view of Mary, Turkmenistan

Boundary between cities and desert

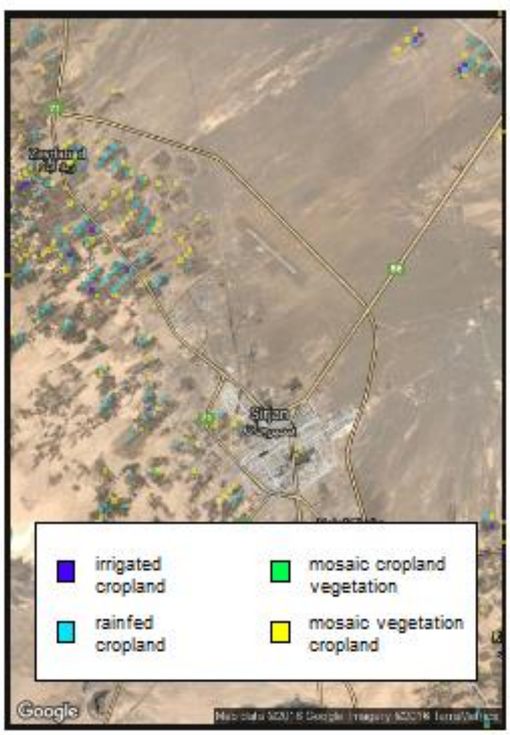

S7: Cropland in Sirjan, south-east Iran

S8: Satellite view of Sirjan, south-east Iran

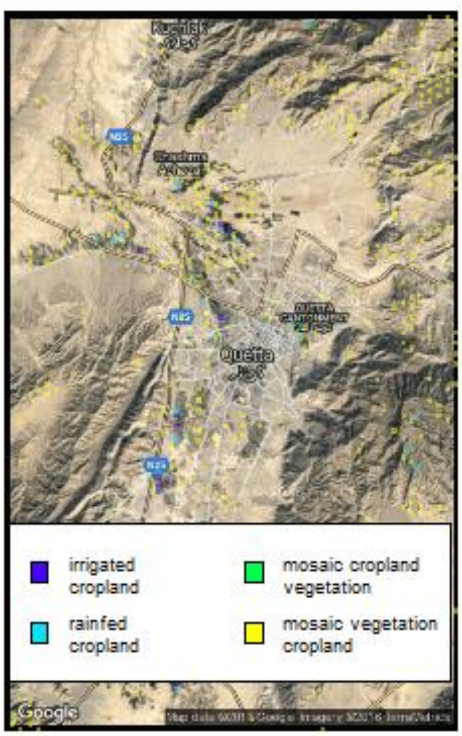

S9: Cropland in Quetta, Balochistan province, Pakistan

S10: Satellite view of Quetta, Balochistan province, Pakistan

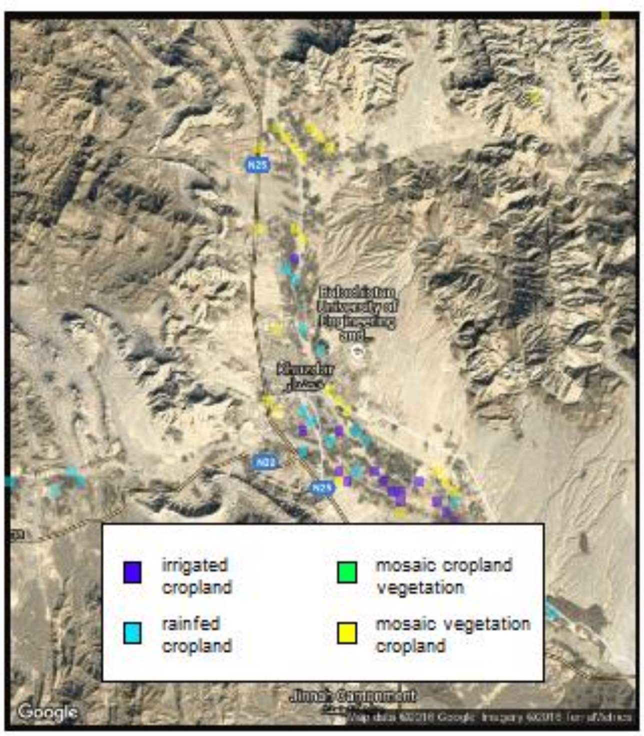

S11: Cropland in Khuzdar, Balochistan province, Pakistan

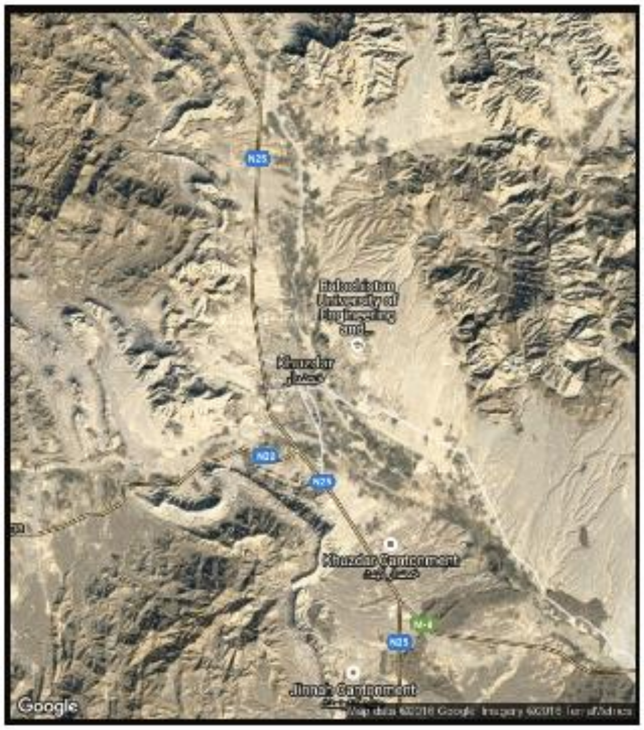

S12: Satellite view of Khuzdar, Balochistan province, Pakistan

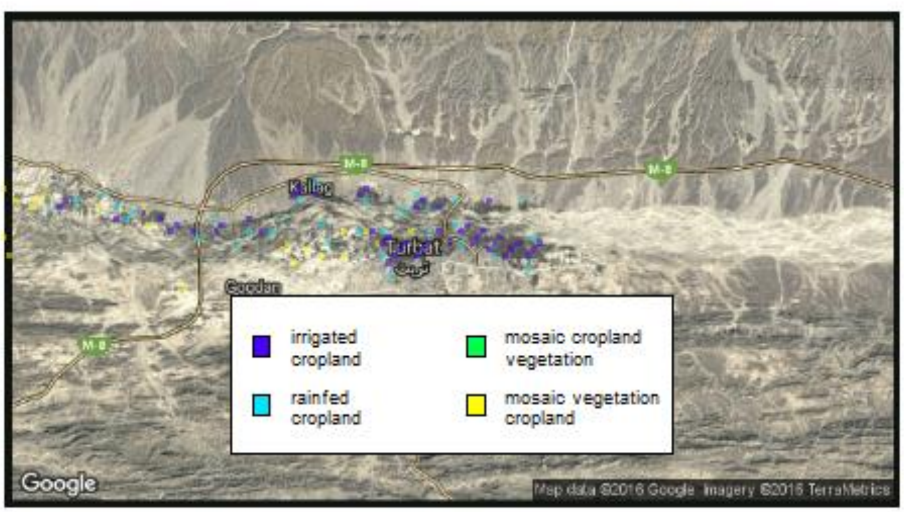

S13: Cropland in Turbat, Balochistan province, Pakistan

S14: Satellite view of Turbat, Balochistan province, Pakistan

Artificial surfaces

High population cities

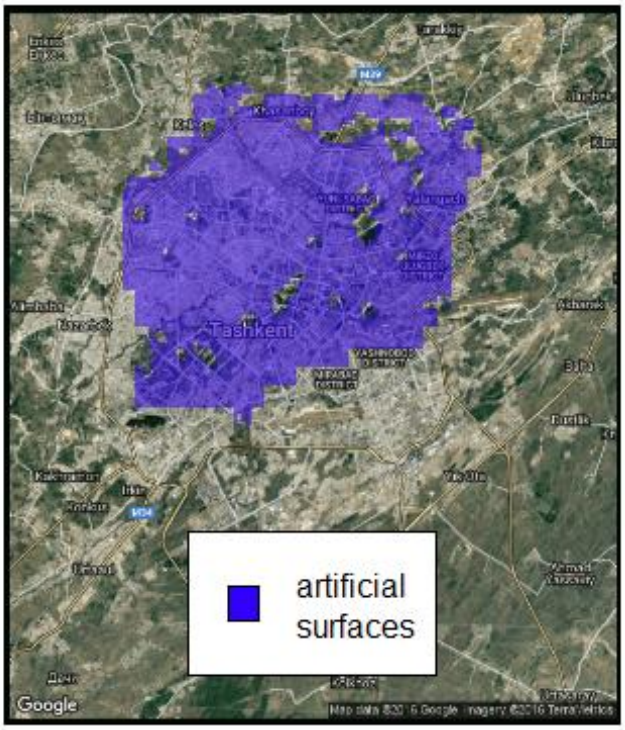

S15: Artificial surfaces in Tashkent, Uzbekistan

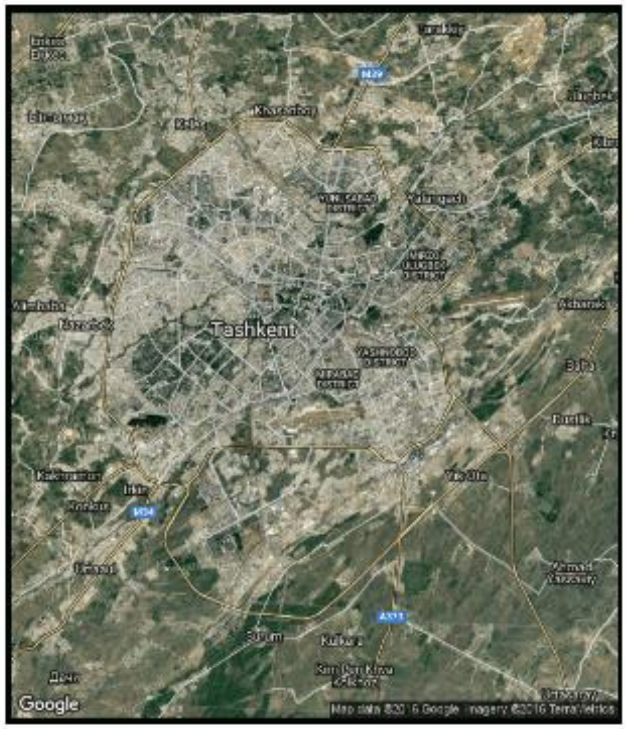

S16: Satellite view of Tashkent, Uzbekistan

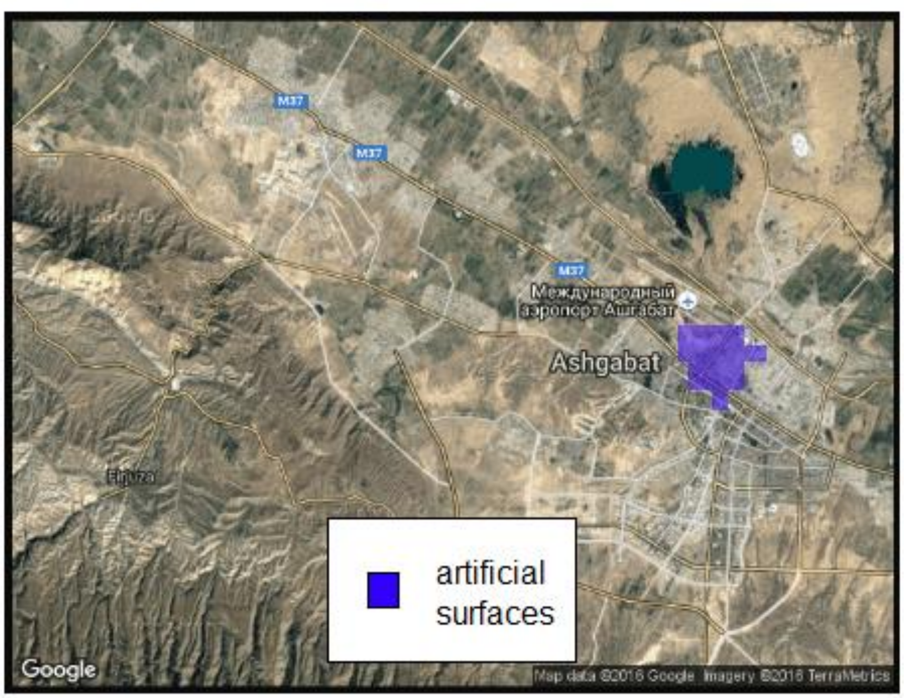

S17: Artificial surfaces in Ashgabat, Turkmenistan

S18: Satellite view of Ashgabat, Turkmenistan

Low population cities

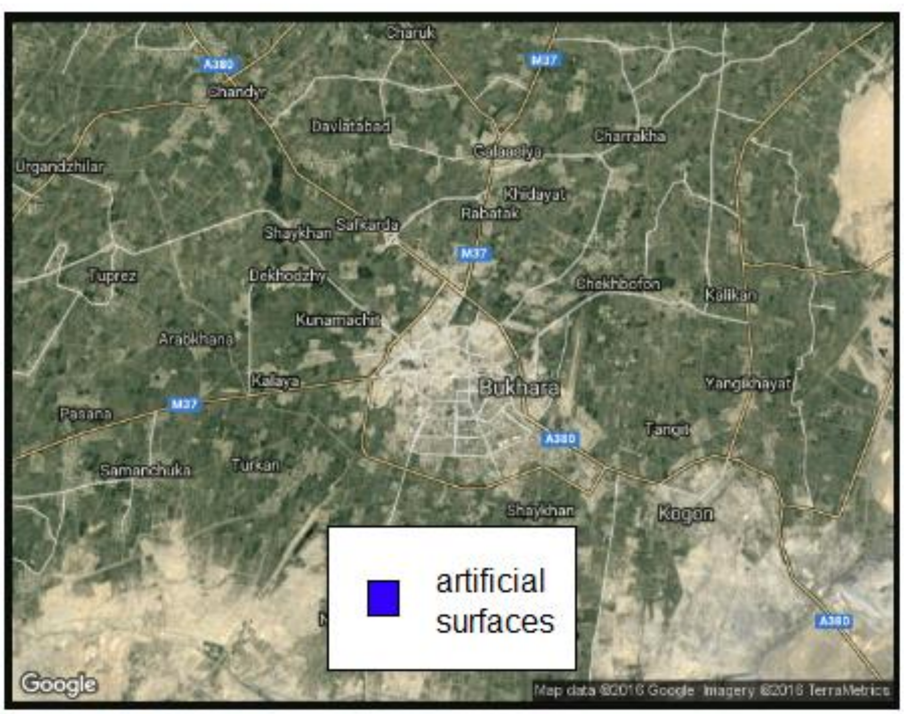

S19: Artificial surfaces in Bukhara, Uzbekistan

S20: Satellite view of Bukhara, Uzbekistan

S21: Artificial surfaces in Turkmenabat, Turkmenistan

S22: Satellite view of Turkmenabat, Turkmenistan

Waterbodies

Saltpans

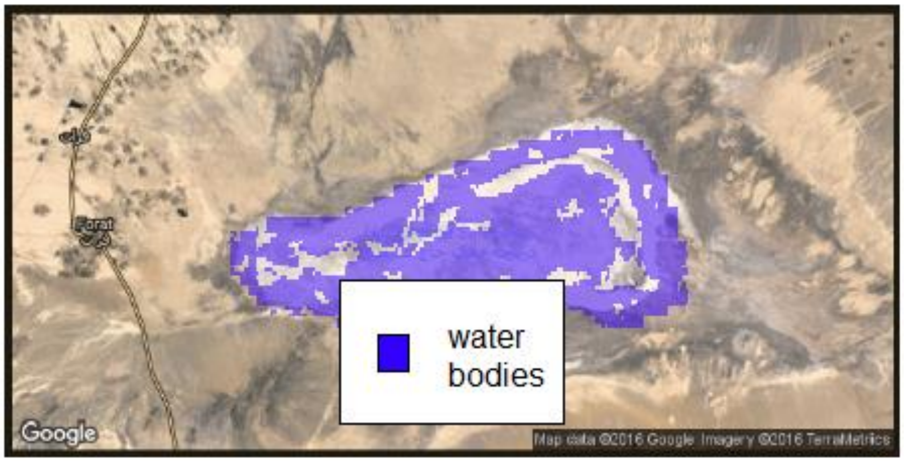

S23: Waterbody classification of Haj Aligholi saltpan, northern Iran

S24: Satellite view of Haj Aligholi saltpan, northern Iran

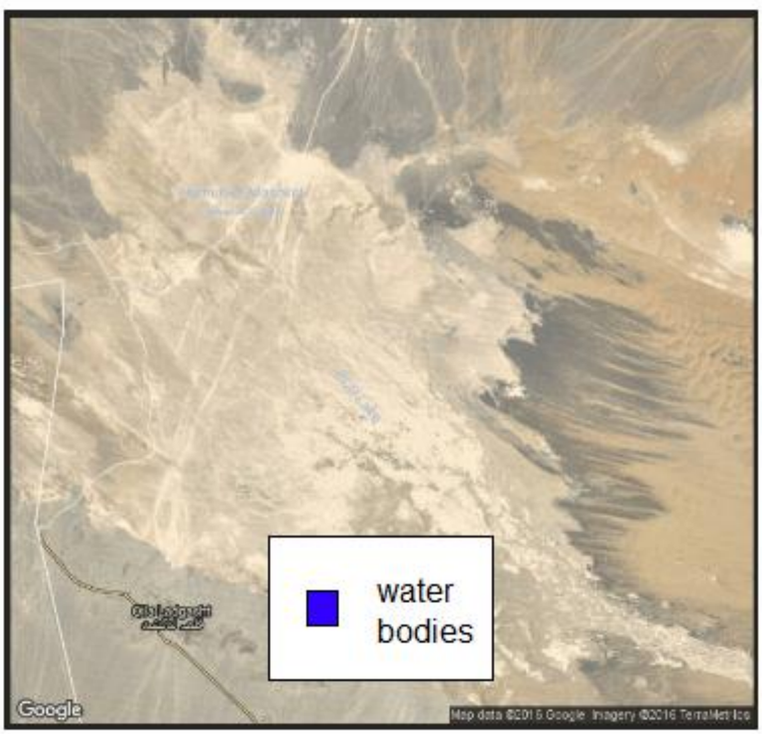

S25: Waterbody classification of a saltpan near the Regional Cooperation for Development Highway, western Balochistan province, Pakistan

S26: Satellite view of a saltpan near the Regional Cooperation for Development Highway, western Balochistan province, Pakistan

Lakes

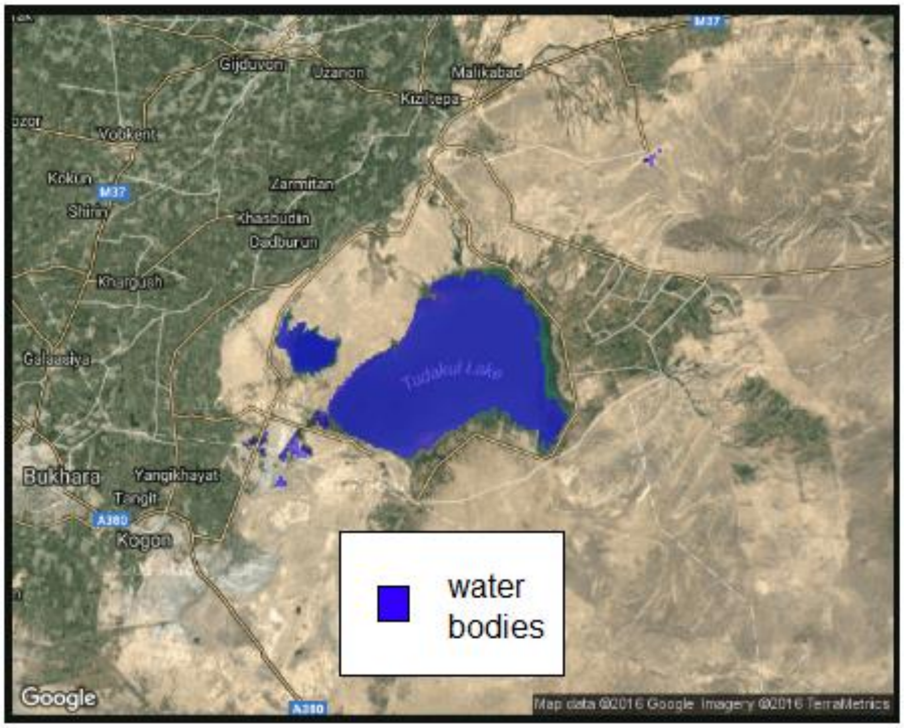

S27: Waterbody classifcation of Tudakul Lake, east of Bukhara, Uzbekistan

S28: Satellite view of Tudakul Lake, east of Bukhara, Uzbekistan

Rivers

S29: Waterbody classifcation of the Amu Darya near Turkmenabat, Turkmenistan

S30: Satellite view of the Amu Darya near Turkmenabat, Turkmenistan

Permanent snow and ice

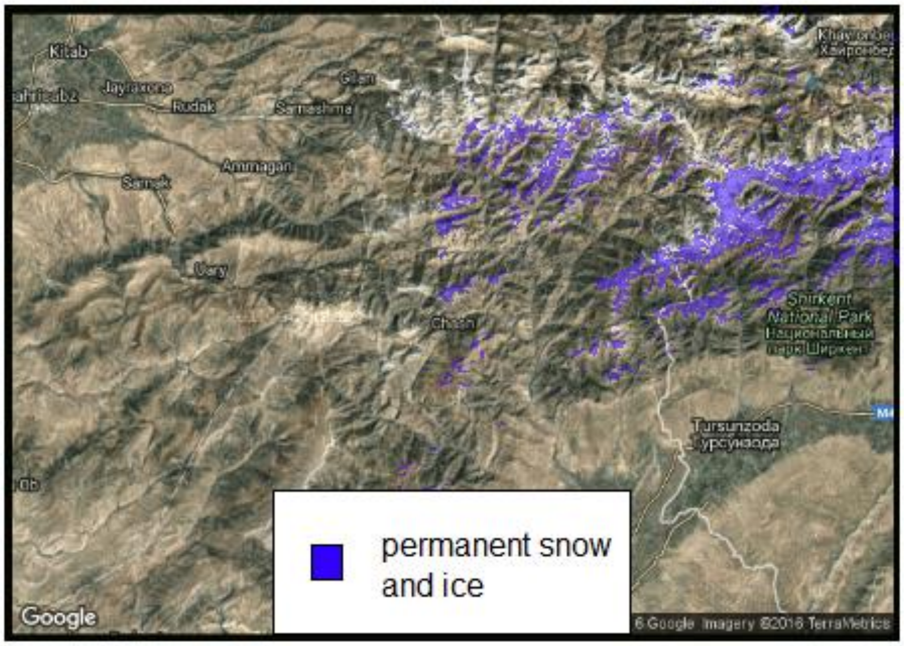

S31: Permanent snow and ice near the Uzbekistan–Tajikistan border

S32: Satellite view of the Uzbekistan–Tajikistan border

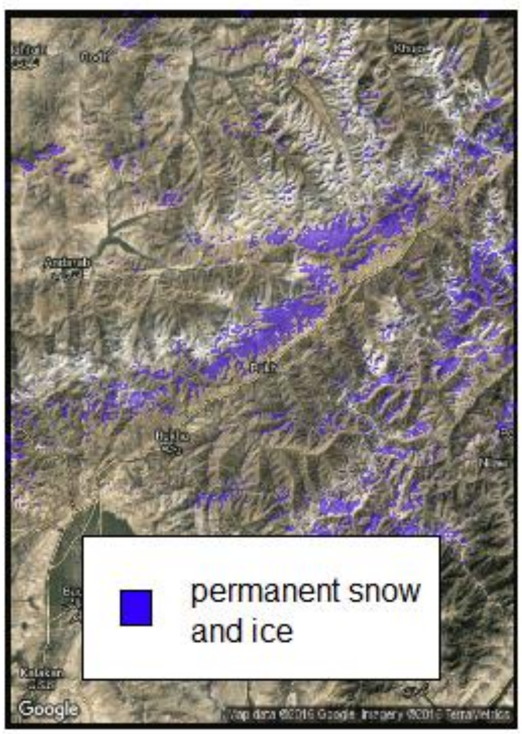

S33: Permanent snow and ice in north-east Afghanistan

S34: Satellite view of north-east Afghanistan

Classification	Percent cover
Post-flooding or irrigated croplands (or aquatic)	7.6
Rainfed croplands	1.7
Mosaic cropland (50-70%) / vegetation (grassland/shrubland/forest) (20–50%)	3.6
Mosaic vegetation (grassland/shrubland/forest) (50–70%) / cropland (20–50%)	7.1
Closed to open (>15%) broadleaved evergreen or semi-deciduous forest (>5m)	0
Closed (>40%) broadleaved deciduous forest (>5m)	0.4
Open (15–40%) broadleaved deciduous forest/woodland (>5m)	0
Closed (>40%) needleleaved evergreen forest (>5m)	0.1
Open (15–40%) needleleaved deciduous or evergreen forest (>5m)	0
Closed to open (>15%) mixed broadleaved and needleleaved forest (>5m)	0.1
Mosaic forest or shrubland (50–70%) / grassland (20–50%)	0.9

Mosaic grassland (50–70%) / forest or shrubland (20–50%)	1
Closed to open (>15%) (broadleaved or needleleaved, evergreen or deciduous) shrubland (<5m)	0.2
Closed to open (>15%) herbaceous vegetation (grassland, savannas or lichens/mosses)	5.9
Sparse (<15%) vegetation	6.6
Closed (>40%) broadleaved forest or shrubland permanently flooded - Saline or brackish water	0
Closed to open (>15%) grassland or woody vegetation on regularly flooded or waterlogged soil - Fresh, brackish or saline water	0
Artificial surfaces and associated areas (Urban areas >50%)	0.1
Bare areas	61.9
Water bodies	1.4
Permanent snow and ice	1.3

S35: Percent cover of land use / cover classes in area of interest (Bontemps et al., 2011).

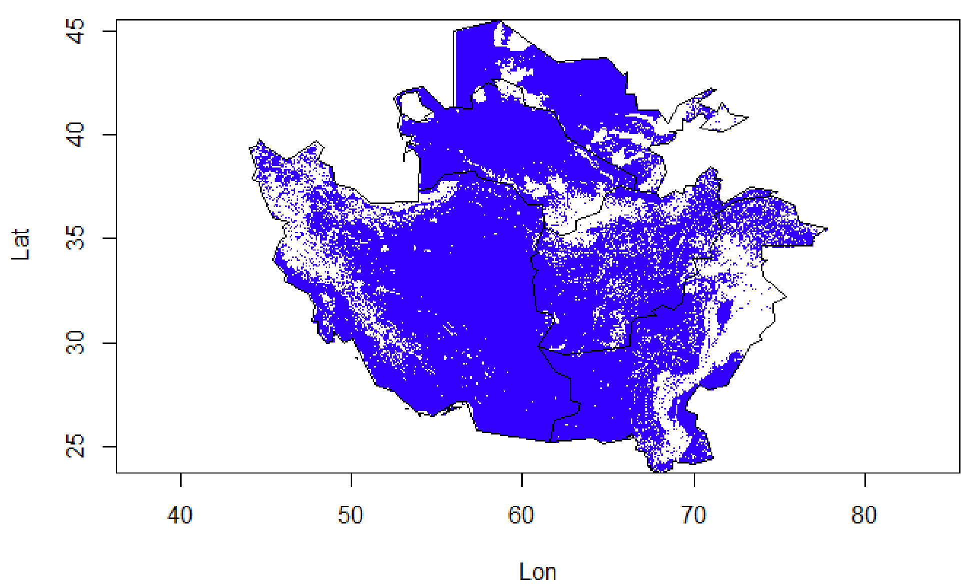

781 S36: Land use / cover mask at 1 km spatial grain with croplands, artificial surfaces, water
782 bodies, and snow / ice excluded (unshaded) (Bontemps et al., 2011).

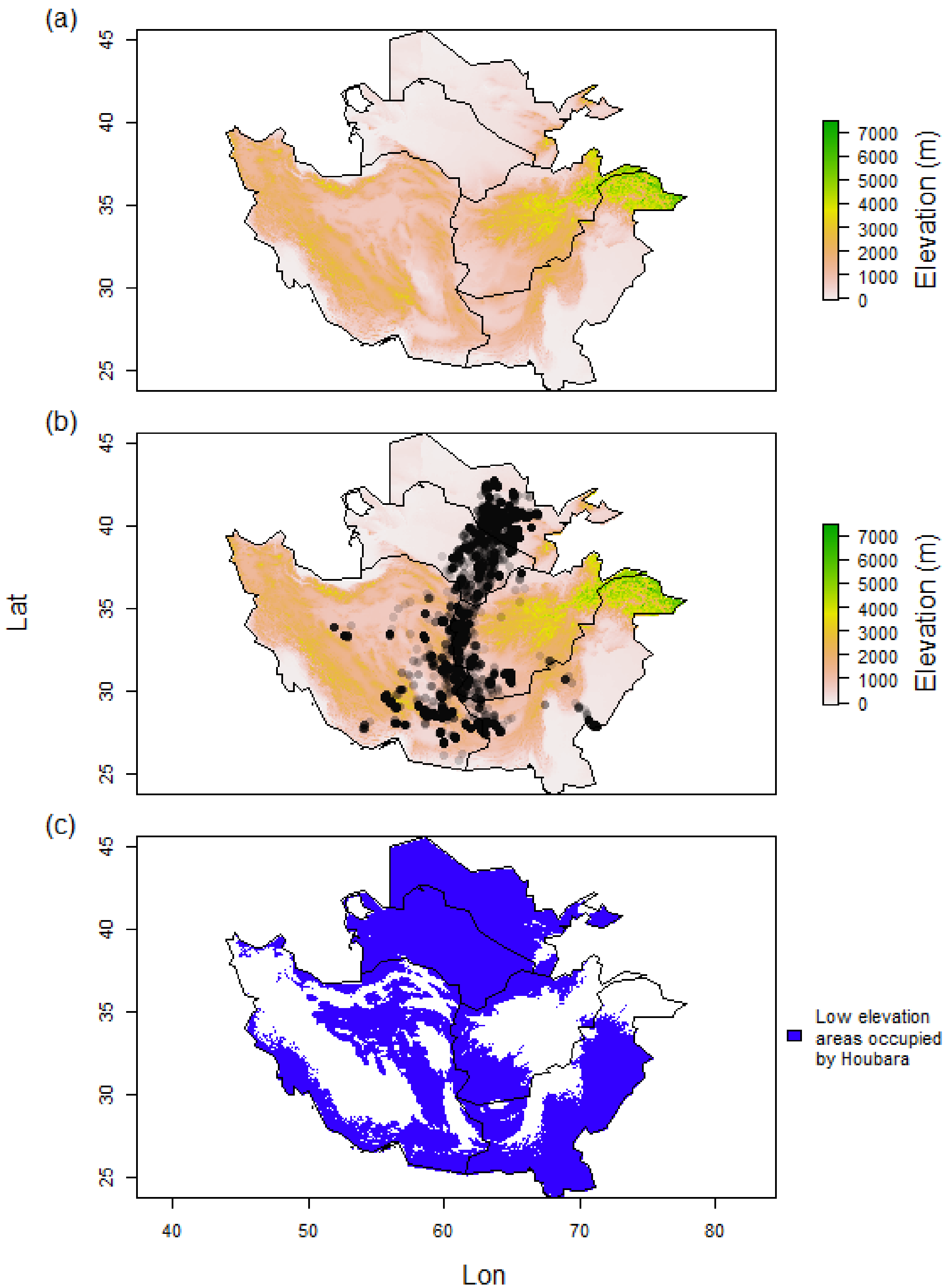

783

S37: Map of (a) elevation at 1 km spatial grain (Jarvis et al., 2015), (b) overlaid with houbara GPS fixes for 61 wild birds from 2011–2016, and (c) resulting mask with areas >1235 m excluded.

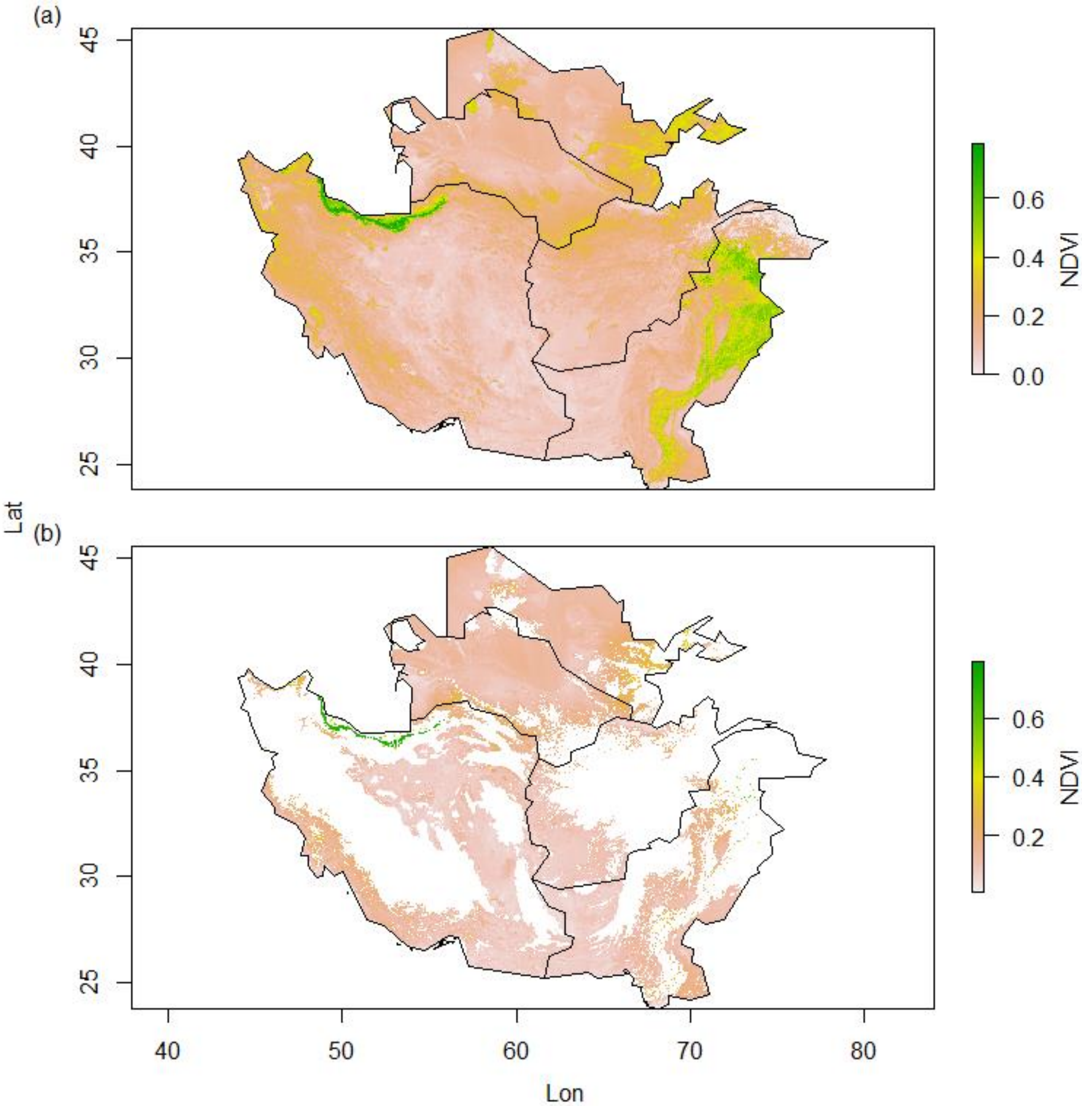

S38: Inter-annual mean of mean annual NDVI across 2000–15 (January–December) (a) at 1 km spatial grain and (b) masked by land use/cover and elevation suitable for houbara.

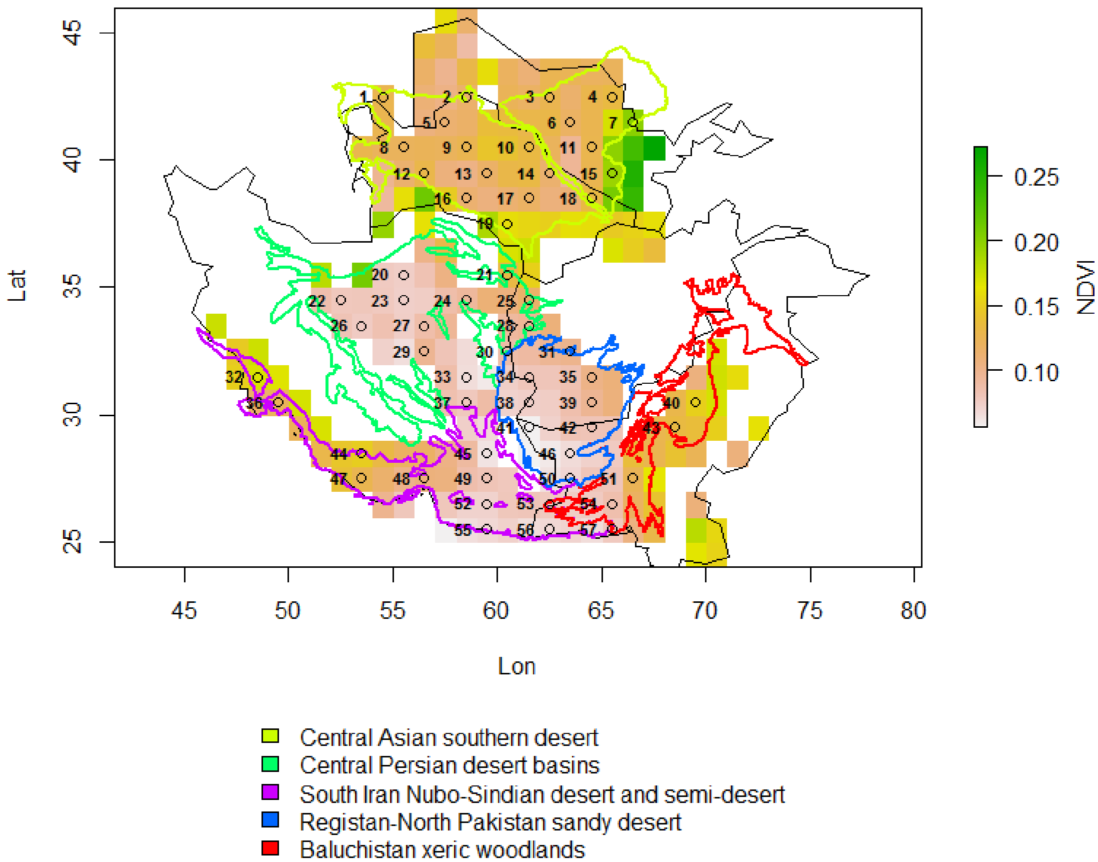

S39: Inter-annual mean of mean annual NDVI from 2000–2015 at 1 degree spatial grain overlaid with WWF ecoregions (Olson et al., 2001).

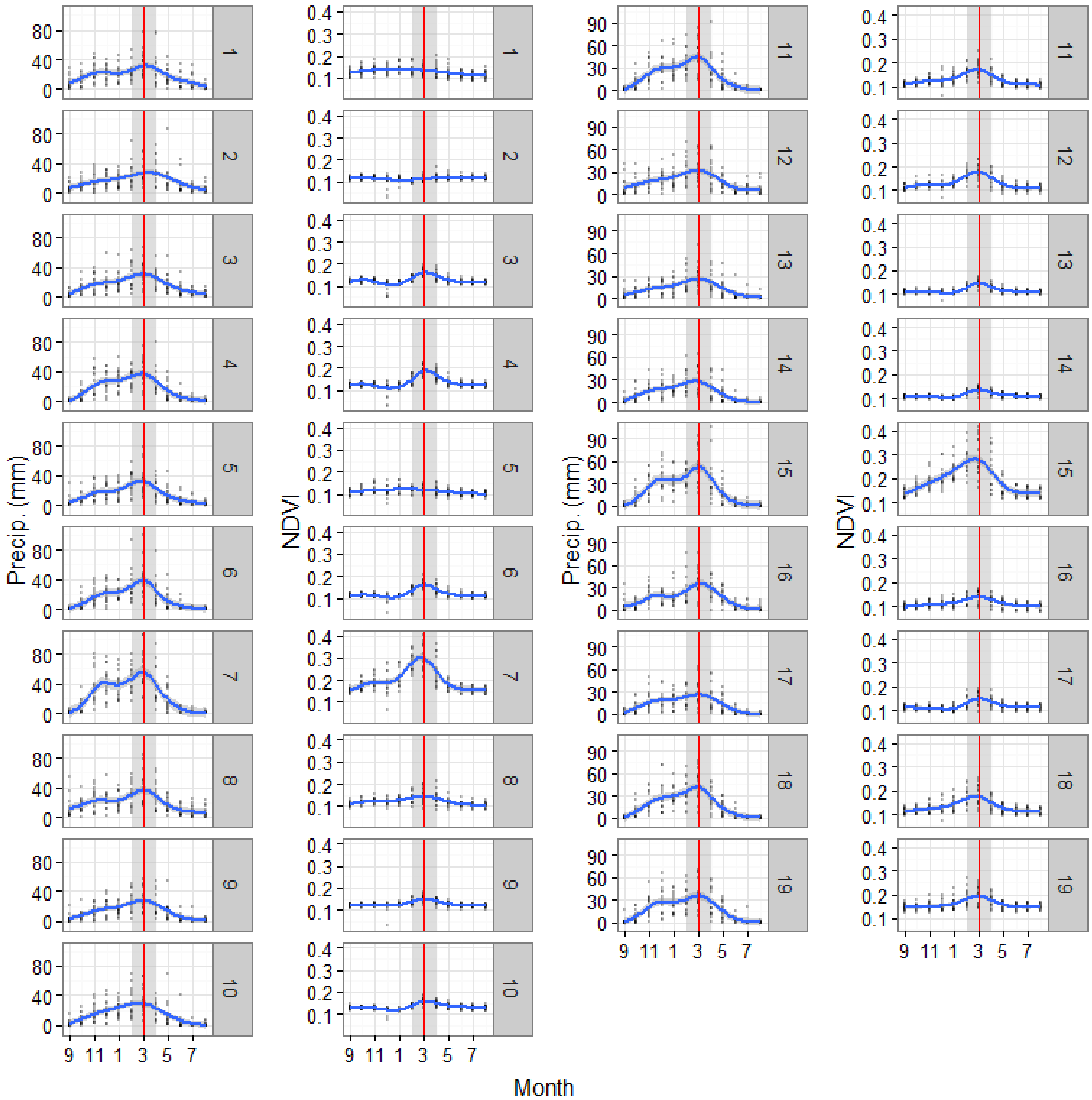

S40: Mean monthly precipitation (mm.month^{-1}) and NDVI (across 2000–2014, late 2015 data unavailable) for degree cells sampled in the Central Asian southern desert. The month axes are offset from minimum to minimum. For reference are a vertical red line at March and gray box from February to May.

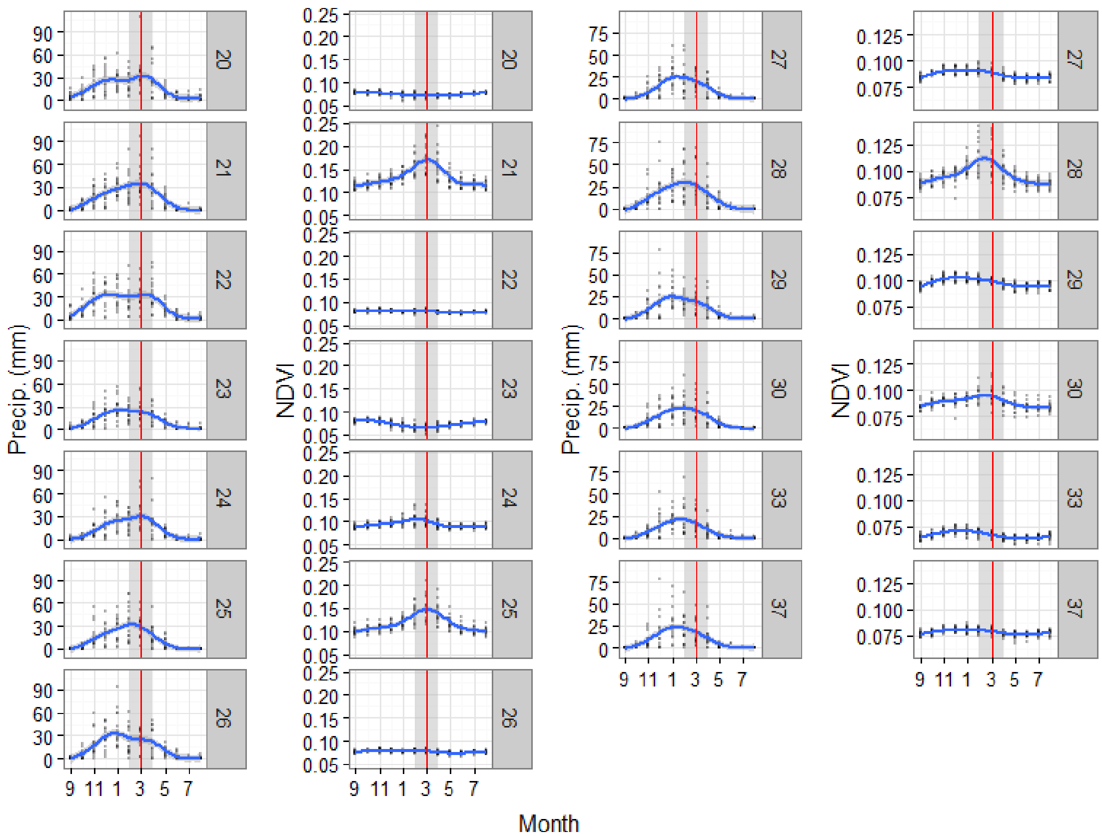

S41: Mean monthly precipitation (mm.month^{-1}) and NDVI (across 2000–2014, late 2015 data unavailable) for degree cells sampled in the Central Persian desert basins. The month axes are offset from minimum to minimum. For reference are a vertical red line at March and gray box from February to May.

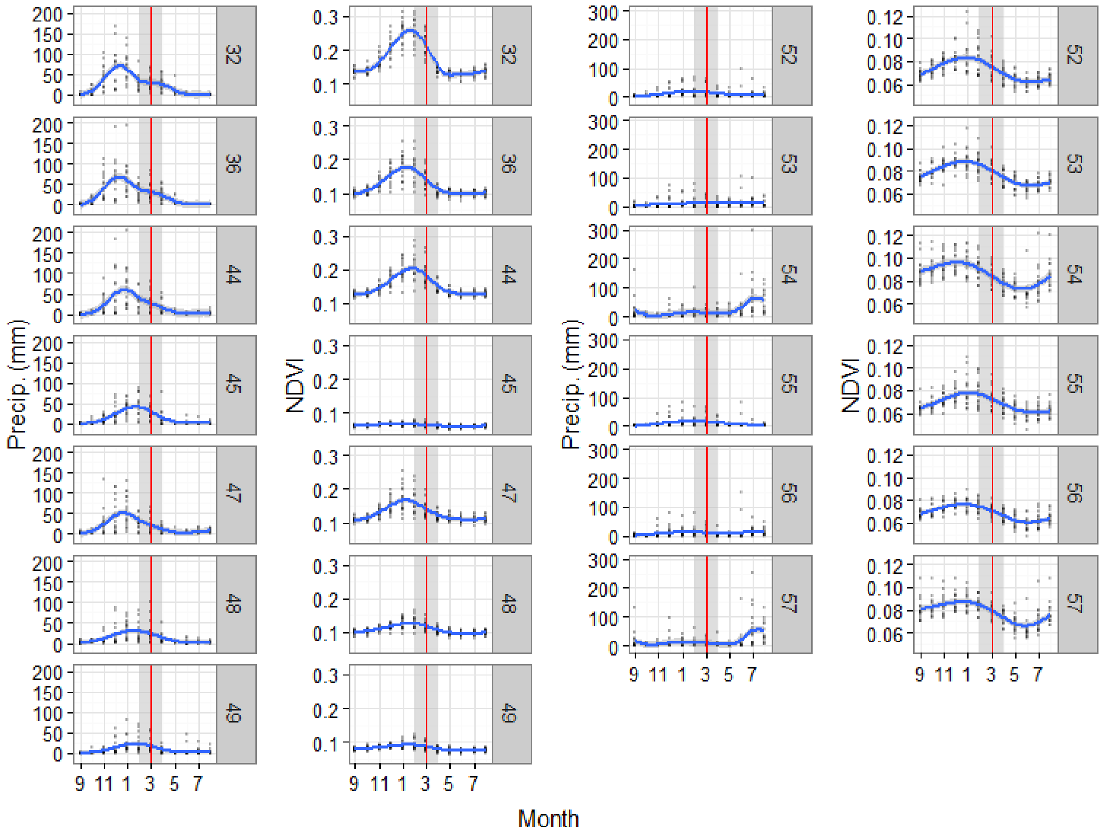

S42: Mean monthly precipitation (mm.month^{-1}) and NDVI (across 2000–2014, late 2015 data unavailable) for degree cells sampled in the South Iran Nubo-Sindian desert and semi-desert. The month axes are offset from minimum to minimum. For reference are a vertical red line at March and gray box from February to May.

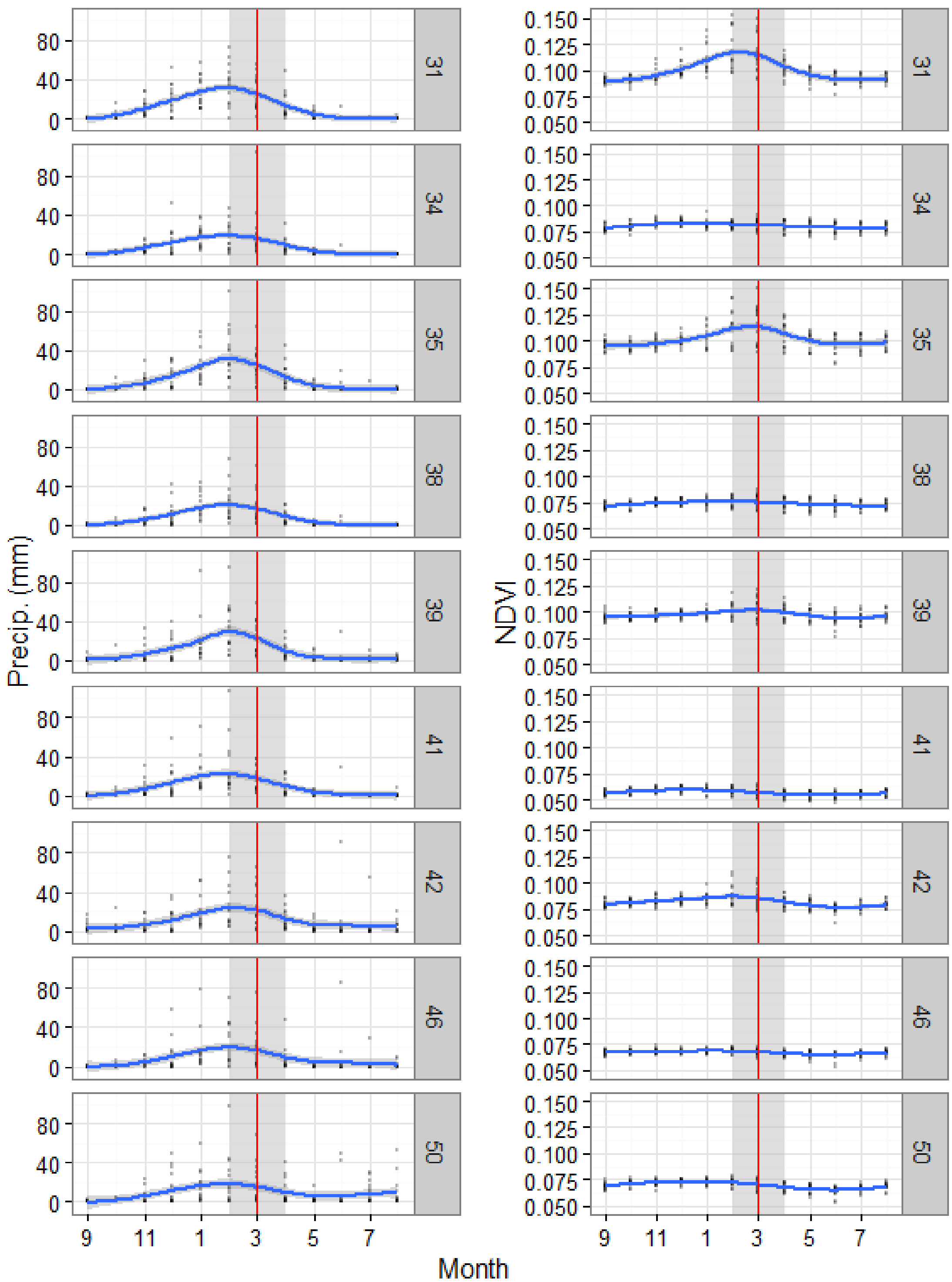

S43: Mean monthly precipitation (mm.month^{-1}) and NDVI (across 2000–2014, late 2015 data unavailable) for degree cells sampled in the Registan-North Pakistan sandy desert. The month axes are offset from minimum to minimum. For reference are a vertical red line at March and gray box from February to May.

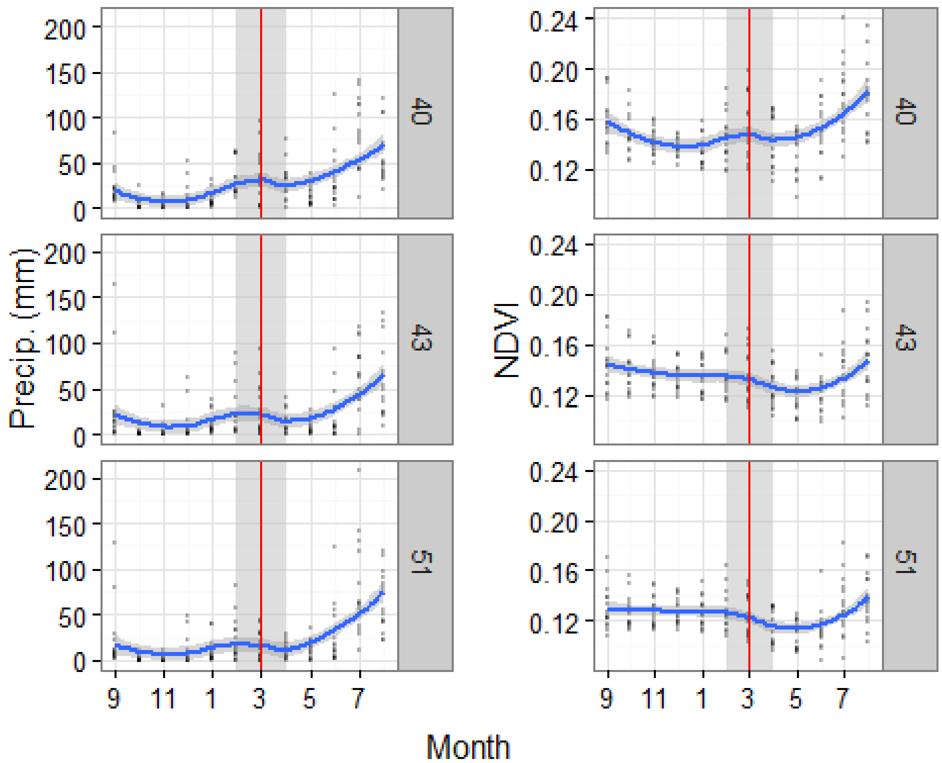

S44: Mean monthly precipitation (mm.month^{-1}) and NDVI (across 2000–2014, late 2015 data unavailable) for degree cells sampled in the Baluchistan xeric woodlands. The month axes are offset from minimum to minimum. For reference are a vertical red line at March and gray box from February to May.

Annual split	Mean adj. R-sq.	SD adj. R-sq.
May-Jun	0.300	0.251
Jun-Jul	0.323	0.240
Jul-Aug	0.323	0.213
Aug-Sep	0.436	0.231
Sep-Oct	0.370	0.214

S45: Mean and standard deviation of adjusted R^2 values of the 244 separate 1 degree cell linear models relating mean annual NDVI to cumulative annual precipitation (2000–2015, n=244) for different annual splits during late spring, summer, and early autumn months.

No. months offset	Mean adj. R-sq.	SD adj. R-sq.
1	0.432	0.228
2	0.428	0.222
3	0.423	0.217
4	0.412	0.213
5	0.183	0.228

S46: Mean and standard deviation of adjusted R^2 values of the 244 separate 1 degree cell linear models relating mean annual NDVI to cumulative annual precipitation (2000–2015, n=244) for different numbers of months annual NDVI is offset ahead of annual precipitation where annual precipitation is considered from August to September.

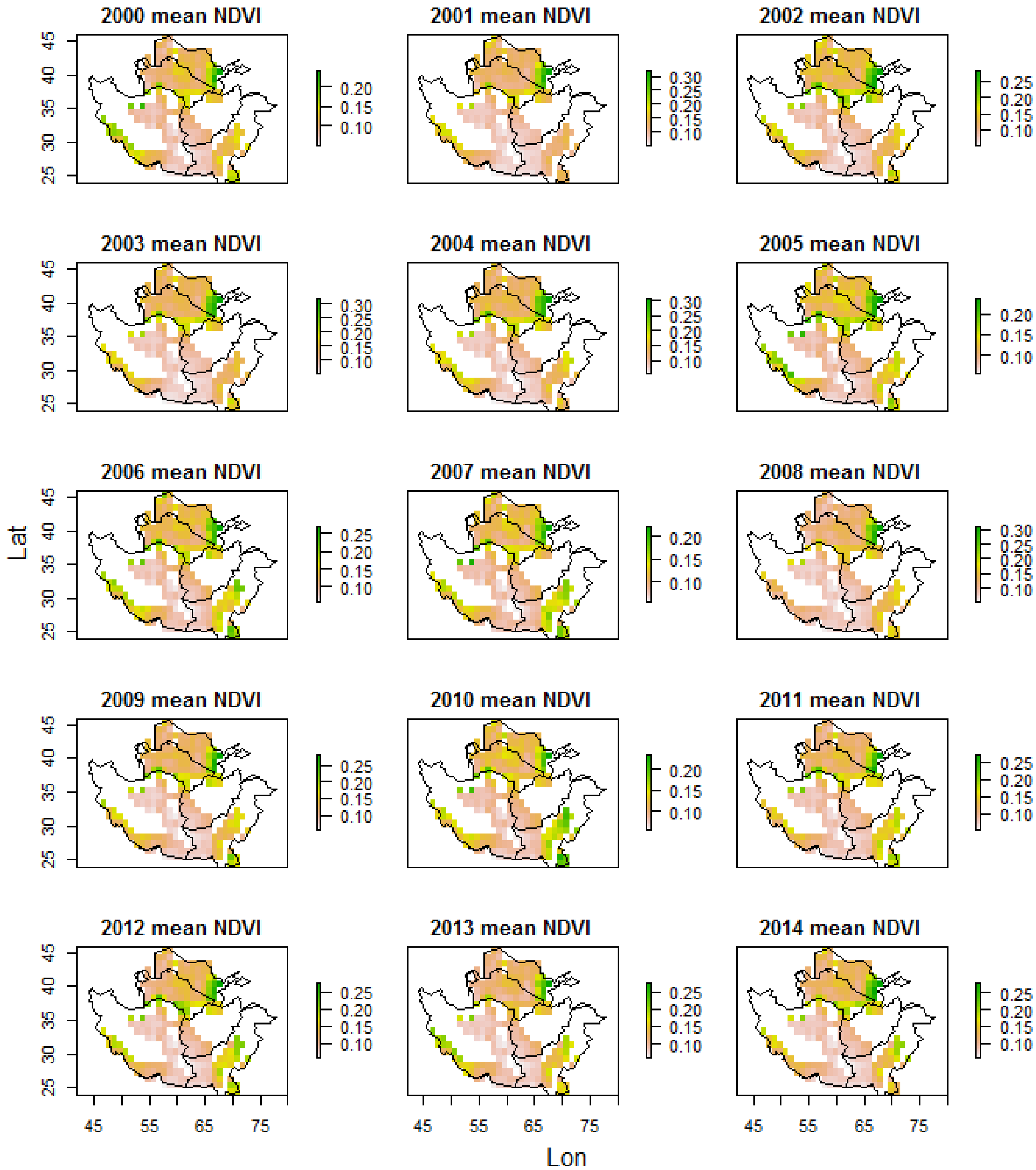

S47: Inter-annual mean of mean annual NDVI by year across 15 annual intervals (split from August to September) spanning 2000-2015 at 1 degree spatial grain masked by land use / cover and elevation.

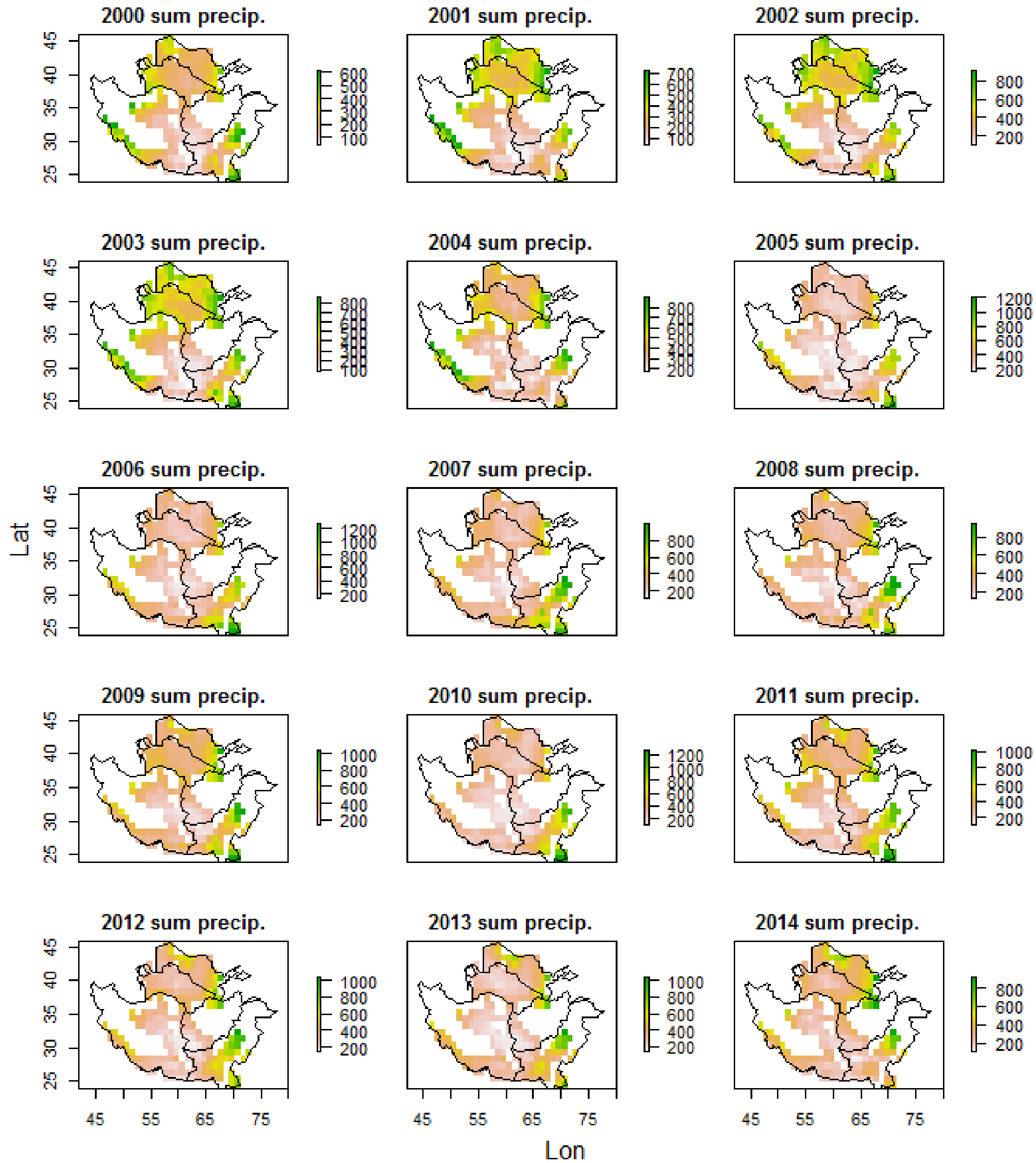

S48: Inter-annual mean of cumulative annual precipitation (mm.yr^{-1}) by year across 15 annual intervals (split from August to September) spanning 2000-2015 at 1 degree spatial grain, masked by land use / cover and elevation.

Variables	VIF
Adj. R-squared	1.4
Slope	2.2
NDVI mean	2.1
Log(x+1) sheep & goats per sq. km	1.4

S49: Variance inflation factors of the adjusted R^2 and slope values of the 244 separate 1 degree cell linear models relating mean annual NDVI to cumulative annual precipitation (2000–2015, n=244) and sheep and goats per square kilometer. All data are masked by unsuitable land use / cover and elevation.

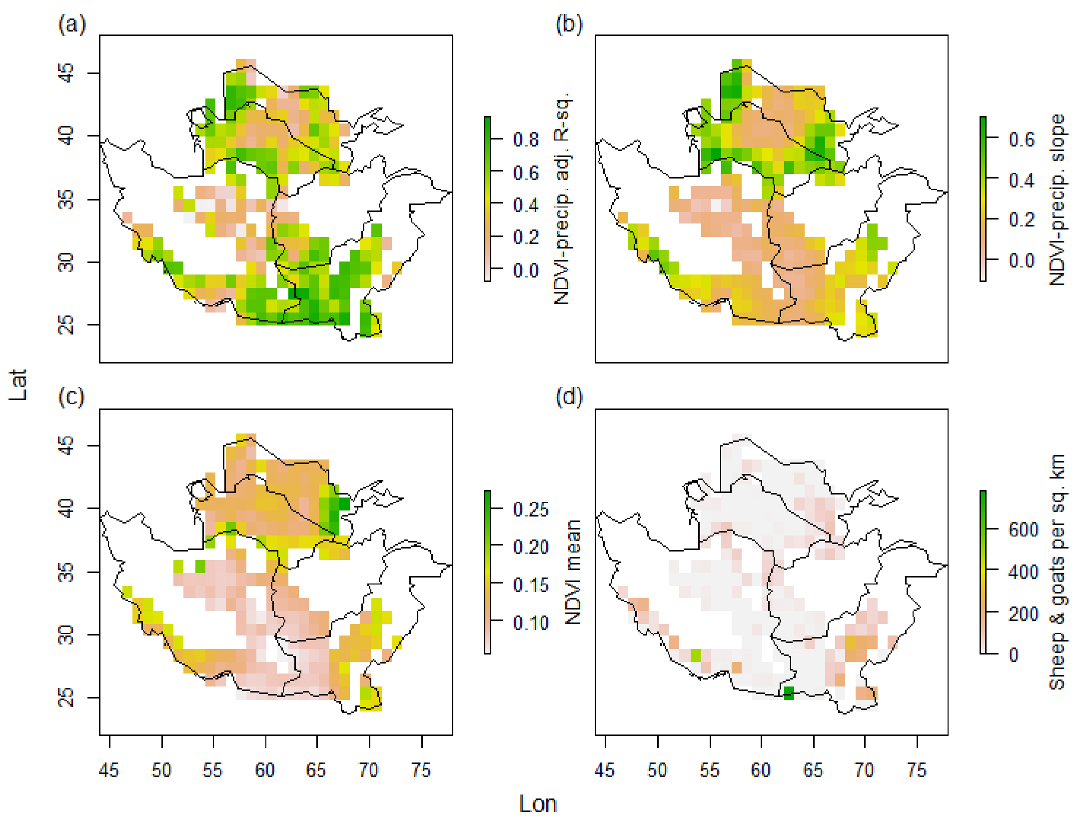

S50: (a) Adjusted R^2 and (b) slope values of the 244 separate 1 degree cell linear models relating mean annual NDVI to cumulative annual precipitation (2000–2015, n=244), (c) inter-annual mean of mean annual NDVI, (d) sheep and goats per square kilometer, and elevation (m) (Wint and Robinson, 2007). All data are mapped at 1 degree spatial grain.

Ecoregion	NDVI mean	NDVI sd	NDVI group	Precip. mean	Precip. sd	Precip. group	Slope mean	Slope sd	Slope group	R-sq mean	R-sq sd	R-sq group
Central Asian southern desert	0.1250	0.0293	a	337	57.3	b	0.2910	0.1540	a	0.430	0.186	b
Central Persian desert basins	0.0897	0.0316	d	273	73.5	c	0.0707	0.0763	c	0.166	0.176	c
South Iran Nubo-Sindian desert and semi-desert	0.0942	0.0385	c	289	79.3	bc	0.1990	0.0910	b	0.544	0.201	a
Registan-North Pakistan sandy desert	0.0817	0.0217	e	195	35.2	d	0.1050	0.0553	c	0.553	0.176	a
Baluchistan xeric woodlands	0.1190	0.0485	b	455	182.0	a	0.2330	0.1070	ab	0.627	0.117	a

S51: Mean, standard deviation, and Tukey HSD groups of cells in each semi-arid ecoregion for the inter-annual mean of (a) mean annual NDVI (January-December) and (b) cumulative annual precipitation across 2000–2015 at 1 km and 1 degree spatial grain, and masked by land use / cover and elevation. Also summarized are the (c) slope and (d) adjusted R^2 values of the 244 separate 1 degree cell linear models relating mean annual NDVI to cumulative annual precipitation (2000–2015, n=244).

Parameters	adj. R^2	χ^2	p
log(precip. mean)	0.48	6.47	<0.001
log(precip. mean), ecoregion	0.62	2.04	<0.001
log(precip. mean), ecoregion, ecoregion: log(precip. mean)	0.62	0.14	0.33

S52: The R^2 of linear models relating log-transformed (to satisfy homoscedasticity) inter-annual mean of mean annual NDVI to inter-annual mean of cumulative annual precipitation (mm.yr^{-1}), ecoregion, and the interaction of ecoregion and mean precipitation at 1 degree spatial grain (n=166), limited to the extent of the five ecoregions across 2000-2015. The χ^2 and p-values show the change in model fit between a given model and the next simplest model based on a χ^2 test of -2 × (log likelihood ratio) of the two nested models with degrees of freedom equal to the number of parameters removed. A significant decrease in model fit on parameter removal indicates that parameter's significance.

	Dependent variable:
	log(NDVI mean)
log(precip. mean)	0.603^{***}
	(0.049)
Constant	-5.712^{***}
	(0.277)
Observations	166
R^2	0.481
Adjusted R^2	0.478
Residual Std. Error	0.206 (df = 164)
F Statistic	152.241^{***} (df = 1; 164)
Note:	$^{*}p<0.05$; $^{**}p<0.01$; $^{***}p<0.001$

S53: Results from the linear model of log-transformed (to satisfy homoscedasticity) inter-annual mean of mean annual NDVI versus inter-annual mean of cumulative annual precipitation (mm.yr^{-1}) at 1 degree spatial grain (n=166), limited to the extent of the five ecoregions across 2000-2015.

	Dependent variable:
	log(NDVI mean)
log(precip. mean)	0.554***
	(0.056)
Ecoregion: Cent. Asia	0.273***
	(0.050)
Ecoregion: Cent. Persia	0.035
	(0.058)
Ecoregion: Regist.	0.117
	(0.070)
Ecoregion: S. Iran	0.030
	(0.057)
Constant	-5.558***
	(0.340)
Observations	166
R^2	0.634
Adjusted R^2	0.622
Residual Std. Error	0.175 (df = 160)
F Statistic	55.330*** (df = 5; 160)
Note:	*p<0.05; **p<0.01; ***p<0.001

S54: Results from the linear model of log-transformed (to satisfy homoscedasticity) inter-annual mean of mean annual NDVI versus inter-annual mean of cumulative annual precipitation (mm.yr^{-1}) and ecoregion at 1 degree spatial grain (n=166), limited to the extent of the five ecoregions across 2000-2015 (Baluchistan as reference level).

	Baluch.	Cent. Asia	Cent. Persia	Regist.	S. Iran
Baluch.	-	<0.001	0.544	0.099	0.599
Cent. Asia	-	-	<0.001	0.003	<0.001
Cent. Persia	-	-	-	0.101	0.909
Regist.	-	-	-	-	0.094
S. Iran	-	-	-	-	-

S55: Raw p-values in pairwise matrix of comparisons between ecoregions (additive effects) from alternating the reference ecoregion in the linear model of mean NDVI versus mean precipitation and ecoregion.

	Baluch.	Cent. Asia	Cent. Persia	Regist.	S. Iran
Baluch.	-	<0.001	1	0.565	1
Cent. Asia	-	-	<0.001	0.022	<0.001
Cent. Persia	-	-	-	0.565	1
Regist.	-	-	-	-	0.565
S. Iran	-	-	-	-	-

S56: Holm-adjusted p-values (to control for table-wide significance) in pairwise matrix of comparisons between ecoregions (additive effects) from alternating the reference ecoregion in the linear model of mean NDVI versus mean precipitation and ecoregion (n=10 unique comparisons between different ecoregions).

	Dependent variable:
	log(NDVI mean)
log(precip. mean)	0.601***
	(0.099)
Ecoregion: Cent. Asia	0.546
	(1.035)
Ecoregion: Cent. Persia	1.469
	(0.883)
Ecoregion: Regist.	0.145
	(1.216)
Ecoregion: S. Iran	-0.408
	(0.892)
Ecoregion: Cent. Asia * log(precip. mean)	-0.045
	(0.176)
Ecoregion: Cent. Persia * log(precip. mean)	-0.253
	(0.153)
Ecoregion: Regist. * log(precip. mean)	0.001
	(0.224)
Ecoregion: S. Iran * log(precip. mean)	0.081
	(0.153)
Constant	-5.838***
	(0.598)
Observations	166
R^2	0.644
Adjusted R^2	0.624
Residual Std. Error	0.175 (df = 156)
F Statistic	31.370*** (df = 9; 156)
Note:	*p<0.05; **p<0.01; ***p<0.001

S57: Results from the linear model of log-transformed (to satisfy homoscedasticity) inter-annual mean of mean annual NDVI versus inter-annual mean of cumulative annual precipitation (mm.yr^{-1}), ecoregion, and the interaction of ecoregion and mean precipitation at 1 degree spatial grain (n=166), limited to the extent of the five ecoregions across 2000-2015 (Baluchistan as reference level).

Parameters	adj. R^2	χ^2	p
NDVI mean	0.39	1.3	<0.001
NDVI mean, ecoregion	0.5	0.41	<0.001
NDVI mean, ecoregion, ecoregion: NDVI mean	0.5	0.04	0.46

S58: The R^2 of linear models relating the slopes of separate 1 degree cell linear models of mean annual NDVI versus cumulative annual precipitation ($mm.yr^{-1}$) (2000–2015, n=166), limited to the extent of the five ecoregions, to inter-annual mean of mean annual NDVI, ecoregion, and the interaction of ecoregion and mean NDVI. The χ^2 and p-values show the change in model fit between a given model and the next simplest model based on a χ^2 test of -2 × (log likelihood ratio) of the two nested models with degrees of freedom equal to the number of parameters removed. A significant decrease in model fit on parameter removal indicates that parameter's significance.

	Dependent variable:
	slope
NDVI mean	2.834^{***}
	(0.277)
Ecoregion: Cent. Asia	-0.105^{***}
	(0.030)
Observations	166
R^2	0.390
Adjusted R^2	0.387
Residual Std. Error	0.111 (df = 164)
F Statistic	104.958^{***} (df = 1; 164)
Note:	$^{*}p<0.05$; $^{**}p<0.01$; $^{***}p<0.001$

S59: Results from the linear model of slopes of separate 1 degree cell linear models relating mean annual NDVI to cumulative annual precipitation ($mm.yr^{-1}$) (2000–2015, n=166) versus inter-annual mean of mean annual NDVI, limited to the extent of the five ecoregions.

	Dependent variable:
	slope
NDVI mean	2.017***
	(0.313)
Ecoregion: Cent. Asia	0.029
	(0.028)
Ecoregion: Cent. Persia	-0.115***
	(0.031)
Ecoregion: Regist.	-0.062
	(0.033)
Ecoregion: S. Iran	0.007
	(0.031)
Constant	0.003
	(0.043)
Observations	166
R^2	0.515
Adjusted R^2	0.500
Residual Std. Error	0.101 (df = 160)
F Statistic	33.937*** (df = 5; 160)
Note:	*p<0.05; **p<0.01; ***p<0.001

S60: Results from the linear model of slopes of separate 1 degree cell linear models relating mean annual NDVI to cumulative annual precipitation ($mm.yr^{-1}$) (2000–2015, n=166) versus inter-annual mean of mean annual NDVI and ecoregion, limited to the extent of the five ecoregions (Baluchistan as reference level).

	Baluch.	Cent. Asia	Cent. Persia	Regist.	S. Iran
Baluch.	-	0.305	<0.001	0.066	0.82
Cent. Asia	-	-	<0.001	0.002	0.376
Cent. Persia	-	-	-	0.047	<0.001
Regist.	-	-	-	-	0.012
S. Iran	-	-	-	-	-

S61: Raw p-values in pairwise matrix of comparisons between ecoregions (additive effects) from alternating the reference ecoregion in the linear model of NDVI-precipitation slope versus mean NDVI and ecoregion.

	Baluch.	Cent. Asia	Cent. Persia	Regist.	S. Iran
Baluch.	-	0.914	0.002	0.263	0.914
Cent. Asia	-	-	<0.001	0.012	0.914
Cent. Persia	-	-	-	0.234	<0.001
Regist.	-	-	-	-	0.074
S. Iran	-	-	-	-	-

S62: Holm-adjusted p-values (to control for table-wide significance) in pairwise matrix of comparisons between ecoregions (additive effects) from alternating the reference ecoregion in the linear model of NDVI-precipitation slope versus mean NDVI and ecoregion (n=10 unique comparisons between different ecoregions).

	Group
Baluch.	bc
Cent. Asia	c
Cent. Persia	a
Regist.	ab
S. Iran	bc

S63: Significant groupings between ecoregions (additive effects) in the linear model of NDVI-precipitation slope versus mean NDVI and ecoregion, based on the holm-adjusted pairwise comparison matrix.

	Dependent variable:
	slope
NDVI mean	2.847***
	(0.738)
Ecoregion: Cent. Asia	0.136
	(0.114)
Ecoregion: Cent. Persia	0.065
	(0.108)
Ecoregion: Regist.	-0.028
	(0.142)
Ecoregion: S. Iran	0.084
	(0.108)
Ecoregion: Cent. Asia * NDVI mean	-0.930
	(0.926)
Ecoregion: Cent. Persia * NDVI mean	-1.772
	(1.002)
Ecoregion: Regist. * NDVI mean	-0.081
	(1.545)
Ecoregion: S. Iran * NDVI mean	-0.645
	(0.977)
Constant	-0.091
	(0.088)
Observations	166
R^2	0.526
Adjusted R^2	0.498
Residual Std. Error	0.101 (df = 156)
F Statistic	19.211*** (df = 9; 156)
Note:	$^{*}p<0.05$; $^{**}p<0.01$; $^{***}p<0.001$

S64: Results from the linear model of slopes of separate 1 degree cell linear models relating mean annual NDVI to cumulative annual precipitation (mm.yr^{-1}) (2000–2015, n=166) versus inter-annual mean of mean annual NDVI, ecoregion, and the interaction of ecoregion and mean NDVI, limited to the extent of the five ecoregions (Baluchistan as reference level).

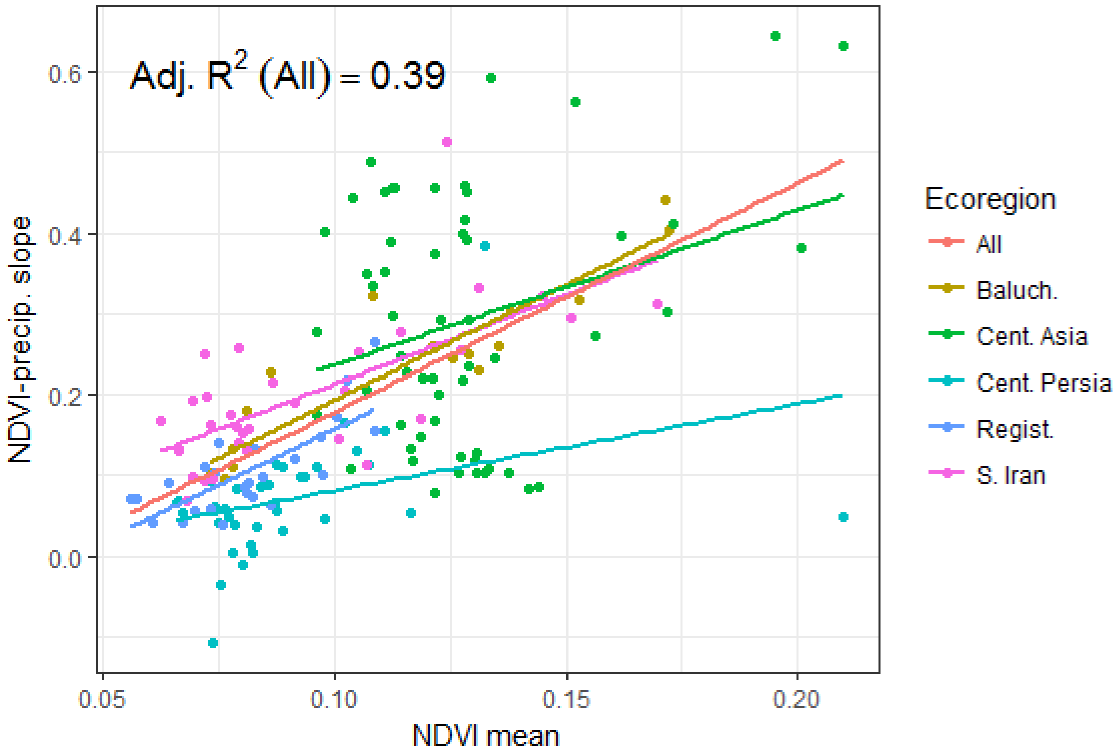

S65: Slopes of separate 1 degree cell linear models relating mean annual NDVI to cumulative annual precipitation ($mm.yr^{-1}$) (2000–2015, n=166) versus inter-annual mean of mean annual NDVI for all cells within the extent of the five ecoregions and cells by ecoregion.